https://doi.org/10.5194/acp-2019-654
Preprint. Discussion started: 4 November 2019

Atmospheric Chemistry and Physics Discussions

Amplification of black carbon light absorption induced by atmospheric aging: temporal variation at seasonal and diel scales in urban Guangzhou

Jia Yin Sun[1,2], Cheng Wu[1,2*], Dui Wu[1,2,3*], Chunlei Cheng[1,2], Mei Li[1,2], Lei Li[1,2], Tao Deng[3], Jian Zhen Yu[4,5,6], Yong Jie Li[7], Qiani Zhou[1,2], Yue Liang[1,2], Tianlin Sun[1,2], Lang Song[1,2], Peng Cheng[1,2], Wenda Yang[1,2], Chenglei Pei[8,9,10], Yanning Chen[10], Yanxiang Cen[11], Huiqing Nian[11], Zhen Zhou[1,2*]

[1]Institute of Mass Spectrometry and Atmospheric Environment, Jinan University, Guangzhou 510632, China
[2]Guangdong Provincial Engineering Research Center for on-line source apportionment system of air pollution, Guangzhou 510632, China
[3]Institute of Tropical and Marine Meteorology, CMA, Guangzhou 510080, China
[4]Department of Chemistry, Hong Kong University of Science & Technology, Hong Kong, China
[5]Division of Environment & Sustainability, Hong Kong University of Science & Technology, Hong Kong, China
[6]Atmospheric Research Center, HKUST Fok Ying Tung Research Institute, Guangzhou 511400, China
[7]Faculty of Science and Technology, University of Macau, China
[8]State Key Laboratory of Organic Geochemistry and Guangdong Key Laboratory of Environmental Protection and Resources Utilization, Guangzhou Institute of Geochemistry, Chinese Academy of Sciences, Guangzhou 510640, China
[9]University of Chinese Academy of Sciences, Beijing 100049, China
[10]Guangzhou Environmental Monitoring Center, Guangzhou 510030, China
[11]Guangzhou Hexin Analytical Instrument Limited Company, Guangzhou 510530, China

Correspondence to: Cheng Wu (wucheng.vip@foxmail.com), Dui Wu (wudui.vip@foxmail.com) and Zhen Zhou (zhouzhen@gig.ac.cn)

https://doi.org/10.5194/acp-2019-654
Preprint. Discussion started: 4 November 2019

Atmospheric Chemistry and Physics Discussions

Abstract. Black carbon (BC) is an important climate forcer in the atmosphere. Amplification of light absorption can occur by coatings on BC aerosols, an effect that remains one of the major sources of uncertainties for accessing the radiative forcing of BC. In this study, the absorption enhancement factor (E_{abs}) was quantified by the minimum R squared (MRS) method using elemental carbon (EC) as the tracer. Two field campaigns were conducted in urban Guangzhou at the Jinan university super site during both wet season (July 31–September 10, 2017) and dry season (November 15, 2017–January 15, 2018) to explore the temporal dynamics of BC optical properties. The average concentration of EC was 1.94±0.93 and 2.81±2.01μgC m^{-3} in the wet and dry seasons, respectively. Mass absorption efficiency at 520 nm by primary aerosols (MAE_{p520}) determined by MRS exhibit a strong seasonality (8.6 m^2g^{-1} in the wet season and 16.8 m^2g^{-1} in the dry season). E_{abs520} was higher in the wet season (1.51±0.50) and lower in the dry season (1.29±0.28). Absorption Ångström exponent ($AAE_{470\text{-}660}$) in the dry season (1.46±0.12) were higher than that in the wet season (1.37±0.10). Collective evidence showed that the active biomass burning (BB) in dry season effectively altered optical properties of BC, leading to elevated MAE, MAE_p and AAE in dry season comparing to those in wet season. Diurnal E_{abs520} was positively correlated with $AAE_{470\text{-}660}$ (R^2=0.71) and negatively correlated with the AE33 aerosol loading compensation parameter (k) (R^2=0.74) in the wet season, but these correlations were significantly weaker in the dry season, which may be related to the impact of BB. This result suggests that lensing effect was dominating the AAE diurnal variability during the wet season. The effect of secondary processing on E_{abs} diurnal dynamic were also investigated. The E_{abs520} exhibit a clear dependency on secondary organic carbon to organic carbon ratio (SOC/OC). E_{abs520} correlated well with nitrate, implying that gas-particle partitioning of semi-volatile compounds may potentially play an important role in steering the diurnal fluctuation of E_{abs520}. In dry season, the diurnal variability of E_{abs520} was associated with photochemical aging as evidenced by the good correlation (R^2=0.69) between oxidant concentrations (O_x=O_3+NO_2) and E_{abs520}.

https://doi.org/10.5194/acp-2019-654
Preprint. Discussion started: 4 November 2019

Atmospheric Chemistry and Physics Discussions

1. Introduction

Atmospheric aerosols have received great attention in recent years due to their global climatic effects and environmental effects (Anderson et al., 2003). Carbonaceous aerosols account for a large fraction of the global aerosol mass as the main light-absorbing materials in aerosols (Kanakidou et al., 2005; Bond and Bergstrom, 2006). Black carbon (BC), which originated from incomplete combustion of hydrocarbon fuels (Johansson et al., 2018), is the dominating fraction of light absorbing carbonaceous aerosols. BC is not only an air pollutant that poses threat to the public health (Grahame et al., 2014; Apte et al., 2015), but also an essential climate forcer (Chung and Seinfeld, 2002). The BC burden in the atmosphere increased substantially since Industrial Revolution, as evidenced by the ice core samples (Ruppel et al., 2014). Sediment cores from eastern China marginal seas also suggest that BC flux was strongly associated with human activities (Fang et al., 2018). The environmental impact of BC was elevated by its growing abundance in the atmosphere. BC had been regarded as the third most important climate forcer after carbon dioxide and methane (IPCC, 2013). The lifetime of BC in the atmosphere is shorter (< 1 week) than other greenhouse gases (Lund et al., 2018), but BC still can be subjected to long-range transport and therefore produce large-scale influences (Ramanathan et al., 2007). On a global scale, BC can heat the atmospheric directly owing to its strong light absorption across the solar spectrum (Bond and Bergstrom, 2006), thus contributes to the warming effect (Bond et al., 2013). On a regional scale, radiative forcing of BC lead to glacier melting at high-altitude regions such as the Tibetan Plateau (Ming et al., 2008), causing seasonal water shortages in Asian rivers and affecting Asian monsoons (Menon et al., 2002; Lau et al., 2006). On a local scale, BC can modify planetary boundary layer meteorology that leads to the “dome effect”, and thus enhance local pollution indirectly (Ding et al., 2016; Wilcox et al., 2016). In microscale, BC was found playing a key role in the photochemical aging of soot by initiating the oxidation of OC (Li et al., 2018c). In addition, BC can indirectly affect the climate by altering cloud formation and cloud cover (Nenes et al., 2002; Koch and Del Genio, 2010; Kaufman and Koren, 2006; Albrecht, 1989). Once deposit on ice and snow, BC can reduced the surface albedo, leading to the melting of ice and snow (Gertler et al., 2016; Kopacz et al., 2011; Flanner et al., 2007; He et al., 2018; Hansen and Nazarenko, 2004).

However, large uncertainties still exist in estimating the radioactive forcing of BC (Bond et al., 2013). The gap largely arises from the limited characterization of BC mixing state in the atmosphere (Fuller et al., 1999; Jacobson, 2001; Nordmann et al., 2014). BC is chemically inert, but morphology transformation is unavoidable once emitted into the atmosphere. A recent study suggested that BC restructuring during aging can be divided into two steps (Pei et al., 2018). First, the void of the BC particles will be filled by the aging

https://doi.org/10.5194/acp-2019-654
Preprint. Discussion started: 4 November 2019


Atmospheric Chemistry and Physics Discussions

induced materials. Once filled, further accumulation of organic and inorganic coating materials leads to the growth of particle size. Ma et al. (2013) reported soot restructuring during water evaporation in a laboratory study. Such morphology transformation leads to alternation of BC optical properties, as evidenced by a number of laboratory experiments (Schnaiter et al., 2005; Zhang et al., 2008; Xue et al., 2009; Shiraiwa et al., 2010; Metcalf et al., 2013; Wei et al., 2013; Chen et al., 2015), field studies (Knox et al., 2009; Cappa et al., 2012; Lack et al., 2012b; Liu et al., 2015; Liu et al., 2017a) and numerical studies (Fuller et al., 1999; Bond et al., 2006; Liu et al., 2016a; Zhang et al., 2017; Lefevre et al., 2019). The presence of coating materials on BC leads to the increase of mass absorption efficiency (MAE) through the lensing effect (Schwarz et al., 2008b). Besides coating thickness, the magnitude of light absorption enhancement by the lensing effect also depends on the optical properties of the coating materials. A coating of brown carbon (BrC) can further amplify the light absorption comparing to a transparent coating (Lack and Cappa, 2010). Recent studies suggested that BC mixing state diversity also affects the bulk E_{abs} (Fierce et al., 2016; Matsui et al., 2018; Cappa et al., 2019).

The total BC light absorption (σ_{abs_total}) after aging can be segregated into primary absorption (σ_{abs_pri}) by the BC core and the additional absorption (σ_{abs_aging}) due to the presence of coating:

$$\sigma_{abs\_total} = \sigma_{abs\_pri} + \sigma_{abs\_aging} \quad (1)$$

The key parameter for light absorption enhancement, E_{abs}, can be calculated from:

$$E_{abs} = \frac{\sigma_{abs\_total}}{\sigma_{abs\_pri}} = \frac{MAE_t}{MAE_p} \quad (2)$$

where MAE_t is the MAE of coated BC:

$$MAE_t = \frac{\sigma_{abs\_total}}{EC} \quad (3)$$

and MAE_p represent the MAE of primary emitted BC:

$$MAE_p = \frac{\sigma_{abs\_pri}}{EC} \quad (4)$$

As a result, atmospheric aging process leads to BC E_{abs} larger than 1.

Three technical approaches had been applied for E_{abs} quantification as summarized in Table 1. The first approach is to use a thermal denuder (TD) upstream of the instrument that measures σ_{abs} (e.g. PAS, photo-acoustic spectrometer). By measuring the denuded and ambient sample in rotation with a desired interval (e.g. 5 min), σ_{abs_total} and σ_{abs_pri} can be obtained to determine E_{abs} following Eq.2. Particle loss in TD is unavoidable and need to be accounted for (Burtscher et al., 2001). The advantage of TD is its ability to obtain

https://doi.org/10.5194/acp-2019-654
Preprint. Discussion started: 4 November 2019


Atmospheric Chemistry and Physics Discussions

high-time-resolution data (Cappa et al., 2012; Lack et al., 2012b; Liu et al., 2015; Liu et al., 2017a). But TD has its own limitations. First, TD is not suitable for long-term measurements (e.g. most studies last for a few months). The selection of working temperature is sample depended and varied by sampling sites. As a result, a universal optimal TD working temperature does not exist. If the temperature is to low, the coating materials cannot be fully vaporized. On the other hand, if the temperature is too high, pyrolysis would occur (Irwin et al., 2013), leading to a biased E_{abs} measurement. For example, Li et al. (2018a) explore the variability of TD temperature on E_{abs} determination in Hong Kong. For a TD temperature of 50°C to 200°C, E_{abs} ranges from 1.02 to 1.20. E_{abs} reaches 1.6 for a TD temperature 280°C. Third, the TD is not the ideal time machine for reversing the morphology transformation of BC. Previous studies have shown that the chain-like-aggregate morphology of nascent BC cannot be restored after thermodenuding of the coatings on the reconstructed BC core, which tends to be more compact and spherical (Bambha et al., 2013; Ghazi and Olfert, 2013). In addition, the high cost of TD-PAS system thwarts its wider applications in field studies.

The second approach for E_{abs} determination is aerosol filter filtration-dissolution (AFD). AFD remove coatings on BC using water and organic solvent (Cui et al., 2016b). The advantage of AFD is that this method can be applied on historical filters archived by long-term/large-scale speciation sampling networks. It opens up a new path to retrieve the historical E_{abs} from datasets with large temporal and spatial coverage. The limitation mainly arises from the AFD treatment process, which only removes the soluble part of the coating. The AFD treatment process is also labor intensive. The time resolution of E_{abs} by AFD depends on the interval of filter sampling, which has a typical sampling time of 24 hr, making it difficult to study the diurnal pattern of E_{abs}.

The third approach is MAE method. E_{abs} is quantified from the ratio of MAE_t to MAE_p as shown in Eq. 2. Since MAE_t can be obtained from ambient measurements, the determination of MAE_p is the key to this approach. One way is to adopt empirical MAE_p in the literature (Cui et al., 2016a). Since the real-world MAE_p could be highly diverse by different sources and varies temporally and spatially (Roden et al., 2006; Adler et al., 2010; Shen et al., 2013; McMeeking et al., 2014; Healy et al., 2015; Cheng et al., 2016; Weyant et al., 2016; Dastanpour et al., 2017; Radney et al., 2017; Conrad and Johnson, 2019), empirical MAE_p at one site might not be applicable at other sites.

Another method to determine MAE_p is combing σ_{abs_total} measurement with a single-particle soot photometer (SP2) to provide the mixing state of BC. The lag time between the incandescence signal and scattering can be used to differentiate thickly coated BC and bare BC. The intercept of linear regression between MAE (y axis) against the number fraction of aged BC (r_{aged}, x axis) represents MAE_p (Lan et al.,

https://doi.org/10.5194/acp-2019-654
Preprint. Discussion started: 4 November 2019

Atmospheric Chemistry and Physics Discussions

2013; Wang et al., 2014). This method only considers E_{abs} dependency on the number fraction of aged particles and ignores the coating thickness of the aged particles, thus is only valid for a limited period of time when coating thickness and size distribution is relatively stable. An improved method for MAE_p determination by SP2 is utilizing the rBC size distribution to calculate the MAE_p by Mie model (Liu et al., 2017a; Wang et al., 2018a; Wang et al., 2018b).

A recently developed approach, Minimum R Squared method (MRS) can be applied to MAE_p determination using elemental carbon (EC) as an tracer (Wu et al., 2018). MRS is a statistic approach and MAE_p can be determined in a quantitative manner that minimizes the arbitrariness in MAE_p estimation by the traditional approach. As summarized in Table 1, E_{abs} by MRS only requires co-located Aethalometer and time-resolved OC/EC measurements, which had been widely deployed around the globe, making MRS potentially more applicable than the TD approach for determining long-term variations of E_{abs}.

In this paper, E_{abs} was determined by the MRS method using the measurement data in urban Guangzhou, a typical megacity in southern China. The aim of this study is to characterize the diurnal and seasonal patterns light absorption enhancement of BC and its association with photochemical aging and BC mixing state. Abbreviations used in this paper are listed in Table A1 in the appendix.

2. Field measurements and data analysis methods

2.1 Characteristics of the observation site

As shown in Figure 1, sampling of this study was conducted at Jinan University atmospheric (JNU) super site (113.35°E, 23.13°N, 40 meters above sea level), which located in Tianhe District, downtown Guangzhou. The site is on top of the library building and surrounded by teaching and residential areas. The campus was surrounded by three busiest road of the city (Figure S1) and traffic emission is a major source of primary emissions. Guangzhou is located in the southern China and is also the geographical center of Guangdong Province. There are limited industrial pollution sources around the sampling site, thus this site can represent the typical urban environment in the Pearl River Delta (PRD) region.

The subtropical climate of PRD is strongly affected by two monsoon systems: South China Sea (SCS) monsoon and Northeast monsoon. April to May is the transition period of the Northeast monsoon to the SCS monsoon. June to September is the SCS monsoon-dominated period (wet season). The southern prevailing wind brings the clean and humid air masses from the vast ocean. October is the transition period of the SCS monsoon to the Northeast monsoon. November to March is the Northeast monsoon-dominated period (dry season). The northeastern prevailing wind brings polluted air masses from the more economically-developed regions in the eastern Asia. This study included two sampling periods: July 31–September 10 2017 and

https://doi.org/10.5194/acp-2019-654
Preprint. Discussion started: 4 November 2019


Atmospheric Chemistry and Physics Discussions

November 15 2017–January 7 2018, corresponding to wet and dry seasons, respectively.

2.2 Light absorption measurements

A dual–spot Aethalometer (Model AE33, Magee Scientific Company, Berkeley, CA, USA) was used for σ_{abs_total} determination. Aethalometer sampling was performed at a flow rate of 5 L min^{-1} with a 2.5 μm cyclone inlet. A Nafion dryer was used to maintain the RH<40%. The data logging time resolution is 1 minute. AE33 reports results in the form of equivalent BC mass (eBC), which can be used to back-calculate the σ_{abs_total}. MAE values from study by Drinovec et al. (2015) was adopted for σ_{abs_total} back-calculations at different wavelengths. A multiple scattering correction factor C_{ref}=3.29 was used according to a recent study in this region (Qin et al., 2018). As a filter-based method, deposition of light absorbing particles on filter leads to the attenuation of filter transmittance signal, which is proportional to the BC mass concentration. However, as the particle deposition layer gradually increase, light was block at the upper particle layer before reaching the underneath particle layer, resulting the well-known artifact: loading effect. Since the lower layer particles did not contribute to the light attenuation, the linear relationship between BC mass concentration and light attenuation signal was distorted.

The AE33 adopted the "dual spot" design to minimize the loading effect (Drinovec et al., 2015), which is an improvement of the traditional "single spot" correction (Virkkula et al., 2007). Two spots perform the sampling simultaneously. The correction can be implemented for each wavelength by the following two equations,

$$eBC1_{raw} = eBC_{\text{compensated}} \cdot (1 - k \cdot ATN1) \quad (5)$$

$$eBC2_{raw} = eBC_{\text{compensated}} \cdot (1 - k \cdot ATN2) \quad (6)$$

Where $eBC1_{raw}$ and $eBC2_{raw}$ are the uncorrected eBC mass determined by the two spots. $eBC_{\text{compensated}}$ is the corrected eBC concentration to be determined. k is the empirical compensation parameter. $ATN1$ and $ATN2$ are the light attenuation measured at the two spots. The flows of the two spots were maintained at a ratio of 2:1 to achieve differential increase of ATN in a set window of time (e.g. 1 min). Since $BC1_{raw}$, $BC2_{raw}$, $ATN1$ and $ATN2$ are all known variables, $eBC_{\text{compensated}}$ and k can be calculated for each measurement following Eqs. (5) & (6). As shown in Figure S2, $eBC1_{raw}$ and $eBC2_{raw}$ exhibit discontinuity once filter was moved to the next position, which implies biases induced by the loading effect. After the dual spot correction, the discontinuity was minimized substantially (Figure S2).

It is worth noting that in the single spot correction, k was a constant in each spot cycle, which means

https://doi.org/10.5194/acp-2019-654
Preprint. Discussion started: 4 November 2019

Atmospheric Chemistry and Physics Discussions

all $eBC_{\text{compensated}}$ within the same cycle (e.g. a cycle last for several hours) have to share the same k. In contrast, time-resolved k can be determined for individual $eBC_{\text{compensated}}$ in the dual spot correction, which is a useful indicator for the mixing state (Drinovec et al., 2017). Zero test was conducted monthly for data quality control purpose.

The absorption Ångström exponent (AAE) can be determined by the multiwavelength measurement of AE33. AAE is a useful parameter to quantify the wavelength dependency of BC light absorption, as defined by the following equation (Moosmüller et al., 2011):

$$\frac{\sigma_{abs,\lambda 1}}{\sigma_{abs,\lambda 2}} = \left(\frac{\lambda_1}{\lambda_2}\right)^{-AAE} \quad (7)$$

where $\sigma_{abs,\lambda 1}$ and $\sigma_{abs,\lambda 2}$ are the light absorption coefficients at the wavelengths of λ_1 and λ_2. The AAE of freshly emitted soot from vehicular emissions is close to 1 (Bond and Bergstrom, 2006; You et al., 2016). An increase of AAE could occur due to the coating of either BrC or non-absorbing materials. Samples that strongly influenced by BB, which are generally rich in primary BrC, can inflate AAE larger than 2 (Reid et al., 2005; Lewis et al., 2008; McMeeking et al., 2009; Pokhrel et al., 2016). Beside BB influence, an increase of AAE up to 1.5 due to coating of non-absorbing materials on the BC particles had also been observed in both model simulations (Lack and Langridge, 2013) and laboratory experiments (You et al., 2016).

2.3 OC and EC measurements

A filed carbon analyzer (Model RT-4, Sunset Laboratory Inc, Tigard, Oregon, USA) was used for OC and EC determination. The detailed sampling procedures can be found in our previous study (Wu et al., 2019), and only a brief description is given here. The sample was collected in the first 45 minutes of each hour at a flow rate of 8 L min^{-1}. The sample was analyzed in the next 15 minutes using thermo-optical analysis (Huntzicker et al., 1982). In the first stage, OC was vaporized by step-wise heating under helium (He) that provides an oxygen-free environment. In the second stage, carrier gas was shifted to oxygen (2% O_2 in He) to oxidize EC on the filter. The decomposition products of these two stages were converted to carbon dioxide (CO_2) by a manganese dioxide (MnO_2) catalyst, then detected by a non-dispersive infrared absorption (NDIR) detector. The instrument blank was analyzed on a daily basis. Filter was changed every 6 days to minimized the bias due to the accumulation of refractory materials on the filter.

2.4 Single particle mass spectrometry measurements

In the wet season, a Single Particle Aerosol Mass Spectrometry (SPAMS, Hexin Analytical Instrument Co., Ltd., China) was deployed at Jinan university atmospheric super site during 11 to 18 August 2017. In dry season, SPAMS data (15 November 2017 to 27 December 2017) from Guangdong environmental monitoring

https://doi.org/10.5194/acp-2019-654
Preprint. Discussion started: 4 November 2019


Atmospheric Chemistry and Physics Discussions

(GEM) site was used to characterize the EC-containing particles. The GEM site was located south to the JNU site (4 km). The operation principle of SPAMS had been introduced previously (Li et al., 2011), and only a brief introduction is given. The particles are introduced into the vacuum system through an 80 μm critical orifice, and then focused into a particle beam by the aerodynamic lens. As a result, the particles are accelerated to a size-dependent terminal velocity. The flight time of a known distance (6 cm) for individual particles is then detected by two orthogonally-orientated continuous laser beams (Nd:YAG, 532 nm) for particle size determination. Sized particles are individually vaporized and ionized by a 266 nm pulsed laser (Nd:YAG, 0.6 mJ). The generated positive and negative ions are then detected by a Z-shaped bipolar time-of-flight mass spectrometer. SPAMS data analysis was performed by the Computational Continuation Core (COCO, V3.2) toolkit based on the MATLAB software. In total, 327,453 and 2,212,688 particles with both positive and negative mass spectra were determined by the SPAMS in wet and dry season, respectively. Based on the ion marker criteria shown in Table S1, 120,351 and 595,180 EC-containing particles were identified in wet and dry season, respectively. EC-containing particles accounting for 37% and 27% of total detected particles in wet and dry season, respectively, which is comparable with a previous SPAMS study in Guangzhou (Zhang et al., 2015). EC-containing particles were further grouped into two categories, EC-fresh and EC-aged. EC-aged particles were extracted from EC-containing particles using the ion markers with the relative peak area (RPA) threshold listed in Table S1, including -97 $[HSO_4]^-$, -62 $[HNO_3]^-$, -46$[NO_2]^-$, 43$[C_2H_3O]^+$, etc. Once EC-aged particles were defined, the remaining EC-containing particles are considered as EC-fresh particles.

Despite the limitations in chemical composition quantification that associated with the matrix effects induced by laser desorption/ionization, SPAMS is a unique technique that can provide chemical composition on a single particle level. The major advantage of single particle analysis by SPAMS enables the characterization of coating martials exclusively on soot particles (Li et al., 2018b), while bulk analytical techniques are incapable of distinguishing whether the non-EC materials are internally or externally mixed with EC. Relative peak area (RPA), which was defined as the peak area of each marker ion divided by the peak area of total ions, has been recognized as an indicator of the relative amount of a species on a particle (Gross et al., 2000; Jeong et al., 2011; Hatch et al., 2014; Zhou et al., 2016). Therefore, RPA is used in this study for SPAMS data analysis.

2.5 Auxiliary measurements

NO_2 was determined by a chemiluminescence analyzer (Model 42iTL, Thermo Scientific), while O_3 was measured by UV photometric analyzer (Model 49i, Thermo Fisher Scientific, Waltham, MA, USA). Span and zero calibrations for the gas analyzers were performed automatedly on a weekly basis. Meteorological factors

https://doi.org/10.5194/acp-2019-654
Preprint. Discussion started: 4 November 2019

Atmospheric Chemistry and Physics Discussions

were measured by a multi-parameter sensor (Model WXT 520, Vaisala, Vantaa, Finland). The planetary boundary layer height (PBLH) measurements was conducted by a micro-pulse lidar (Sigma Space Co., USA) at the Guangzhou Meteorological Bureau (GMB, 23.00° N, 113.32° E, elevation: 43 m). Hourly backward trajectories for the past 72 hours were calculated using NOAA's HYSPLIT (Hybrid Single Particle Lagrangian Integrated Trajectory, version 4) model (Draxier and Hess, 1998) for both dry wand wet seasons. Backward trajectory cluster analysis was conducted using MeteoInfo (Wang, 2014, 2019). Fire count data from Visible Infrared Imaging Radiometer Suite (VIIRS) on board the Suomi NPP weather satellite (Csiszar et al., 2014) was downloaded from the NASA FIRMS website (https://firms.modaps.eosdis.nasa.gov/) to generate the fire count map.

2.6 MAE_p estimation by MRS method

MAE_p is the key parameter in the E_{abs} calculation. In this study, MAE_p was determined by the newly developed MRS method (Wu et al., 2018), using EC as a tracer. In MRS calculation, the correlation (R^2) between measured EC and estimated σ_{abs_aging} is examined as a function of a series of hypothetical MAE_p (MAE_{p_h}). The atmospheric aging induced additional light absorption, and σ_{abs_aging} can be calculated by subtracting the absorption coefficient of primary aerosols, as shown in Eq.8 (a combination of Eqs. 1&4):

$$\sigma_{abs\_aging} = \sigma_{abs\_total} - MAE_p \times EC \quad (8)$$

The MAE at the minimum R^2 of the EC vs. σ_{abs_aging} relationship corresponds to the authentic MAE_p. The detailed method evaluation of MRS can be found in our previous paper (Wu et al., 2018) . Only a brief description on the calculation steps is provided here. EC from the Sunset carbon analyzer and σ_{abs_total} from AE33 are used as input variables. During the calculation of MAE_p by MRS, MAE_{p_h} is varied continuously in a reasonable range. At each MAE_{p_h}, corresponding hypothetical σ_{abs_aging} ($\sigma_{abs\_aging\_h}$) values are calculated for the dataset and a correlation coefficient value (R^2) of EC vs. $\sigma_{abs\_aging\_h}$ (i.e., R^2(EC, $\sigma_{abs\_aging\_h}$)) is obtained. By searching the MAE_{p_h} in a desired range (e.g. from 0.1 to 50 with an interval of 0.1), a series of R^2(EC, $\sigma_{abs\_aging\_h}$) values are then plotted against the MAE_{p_h} values (Figure 2).

The σ_{abs_pri} is the part of light absorption from primary emitted soot particles. As a result, σ_{abs_pri} is well correlated with EC mass. In contrast, σ_{abs_aging} is the part of light absorption gained during the aging processes after emission. The variability of σ_{abs_aging} mainly depends on the coating thickness of the soot particles. Consequently, σ_{abs_aging} is independent of EC mass and the MAE_{p_h} corresponding to the

https://doi.org/10.5194/acp-2019-654
Preprint. Discussion started: 4 November 2019


Atmospheric Chemistry and Physics Discussions

minimum R^2(EC, $\sigma_{abs\_aging\_h}$) would then represent the authentic MAE_p.

It is worth noting that MAE_p by MRS represents the MAE_p at the emission source, which is conceptionally different from the MAE_p by the TD method. First, the morphology and optical properties of freshly emitted BC particles (chain-like aggregates) is different from that of thermally denuded BC particles (compact aggregates). Second, most of the coatings are removed for TD denuded BC particles, but freshly emitted BC particles usually come with a thin coating of OC formed from condensation of organic vapors due to the temperature gradient from the flame to the ambient air. As a result, the MRS-derived MAE_p is expected to be higher than the MAE_p by the TD method.

2.7 Secondary organic carbon (SOC) estimation by MRS method

OC can be separated into two categories based on the formation nature. Primary organic carbon (POC) can be emitted from traffic emission (Huang et al., 2014), biomass burning (Simoneit, 2002), trash burning and cooking (Mohr et al., 2009). Secondary organic carbon (SOC) can be formed through oxidation of volatile organic compounds (VOCs) or semi-volatile POC (Hallquist et al., 2009). The EC tracer method had been used extensively for SOC estimation (Turpin and Huntzicker, 1995):

$$POC = (OC/EC)_{pri} \times EC + OC_{non-comb} \quad (9)$$

$$SOC = OC_{total} - POC \quad (10)$$

Combing Eqs. (9)&(10):

$$SOC = OC_{total} - (OC/EC)_{pri} \times EC - OC_{non-comb} \quad (11)$$

$(OC/EC)_{pri}$ represents the overall OC/EC ratio of aerosols from primary emission sources, while $OC_{non\text{-}comb}$ represents primary OC from non-combustion process. $OC_{non\text{-}comb}$ can be determined from the intercept of OC vs. EC linear regression. In this study, weighted orthogonal distance regression (WODR) was used to account for errors in both x and y variables (Wu and Yu, 2018). By grouping the data into percentile subsets using OC/EC ratio from the lowest to the highest (1–100%, with an interval of 1%), a series of intercepts were obtained as a function of OC/EC percentile (Figure S3). The intercept term in the OC vs. EC WODR is very small (-0.88 – -0.05) throughout the percentile range (1–100%). Since this term is small, $OC_{non\text{-}comb}$ was set to zero for SOC estimation in this study.

$(OC/EC)_{pri}$ is the key parameter for SOC calculation in the EC tracer method. In MRS method, the correlation (R^2) between measured EC and estimated SOC (from Eq. 10) was examined as a function of a series of hypothetical $(OC/EC)_{pri}$ ($(OC/EC)_{pri\_h}$). The OC/EC ratio at the minimum R^2 (EC vs. SOC)

https://doi.org/10.5194/acp-2019-654
Preprint. Discussion started: 4 November 2019


Atmospheric Chemistry and Physics Discussions

corresponds to the authentic primary OC/EC ratio (Millet et al., 2005). The detailed calculation steps can be found in our previous paper (Wu and Yu, 2016). Only a brief description is given here. In MRS calculation, $(OC/EC)_{pri\_h}$ was varied continuously in a reasonable range (e.g. from 0.1 to 10 with an interval of 0.1). Hypothetical SOC (SOC_h) values were calculated at individual $(OC/EC)_{pri\_h}$ for the whole dataset. A series of R^2 values of EC vs. SOC_h (i.e., $R^2(EC,SOC_h)$) were generated and then plotted against the $(OC/EC)_{pri\_h}$ values. Based on the assumption that variations of EC and SOC are independent, the $(OC/EC)_{pri\_h}$ corresponding to the minimum $R^2(EC,SOC_h)$ would then indicate the authentic $(OC/EC)_{pri}$ ratio.

In our previous work, numerical studies were performed and the results showed that the minimum R squared method (MRS) is more robust in SOC estimation than the minimum OC/EC and percentile OC/EC method (Wu and Yu, 2016). As a result, the MRS method had been gradually adopted for SOC estimation in recent studies (Xu et al., 2018b; Bian et al., 2018; Ji et al., 2018; Ying et al., 2018; Ji et al., 2019; Wu et al., 2019).

An Igor Pro (WaveMet rics, Inc. Lake Oswego, OR, USA) based computer program (Wu and Yu, 2016) was used to implement MRS calculation. Another two Igor Pro-based computer programs, Histbox (Wu et al., 2018) and Scatter Plot (Wu and Yu, 2018), were used for generating the box plots and scatter plots presented in this study. These computer programs (with operation manuals) can be downloaded freely from https://sites.google.com/site/wuchengust.

3. Results and discussions

3.1 Seasonality of carbonaceous aerosols concentrations and optical properties

The time series of EC, OC, optical properties and supporting measurements during the wet and dry seasons are shown in Figure S4. The hourly EC concentrations ranged from 0.43 to 7.40 and 0.54 to 12.04 μgC m^{-3} in wet and dry seasons, respectively. As for OC, the hourly average ranged from 0.32 to 13.84 and 0.51 to 25.31 μgC m^{-3} in wet and dry seasons, respectively. The hourly OC/EC ratios ranged from 0.25 to 6.92 and 0.33 to 8.69 in wet and dry seasons, respectively. In wet season, the wind direction is southeasterly dominated, bringing the relatively clean background air masses from the vast ocean. In dry season, the northeasterly wind prevails, which promotes the long-range transport of air pollutants from the east and central China.

As shown in Figure 1, EC, OC and OC/EC $AAE_{470-660}$ all exhibit clear seasonality. Average EC concentrations (with 1 standard deviation, hereafter) were 1.94±0.93 and 2.81±2.01 μgC m^{-3} in wet and dry seasons, respectively. The EC level was comparable to the measurements made in 2012 at a Guangzhou suburban site (1.67±1.35 μgC m^{-3} in wet season, 3.47±2.75 μgC m^{-3} in dry season) (Wu et al., 2019). Back trajectories analysis showed that in wet season most air masses were from South China Sea, with only 31.67%

https://doi.org/10.5194/acp-2019-654
Preprint. Discussion started: 4 November 2019


Atmospheric Chemistry and Physics Discussions

air masses were locally influenced (Figure S5a). Among the 3 back trajectory clusters in wet season, the locally influenced air masses exhibit the shortest back trajectory (C1), leading to the highest EC concentration (2.01±1.22 μgC m^{-3}). As the back trajectory distance increased from C2 to C3, the corresponding EC decreased from 2.01± 0.88 to 1.56 ± 0.67 μgC m^{-3}. During dry season, air masses were dominated by those of northern origin. EC concentrations also exhibit gradient on the trajectory path length. Long-path (C3) trajectories lead to low EC concentrations (2.01±1.46 μgC m^{-3}), while short-path trajectories lead to higher concentrations (C1: 3.50±2.13 μgC m^{-3}; C2: 2.52±1.91 μgC m^{-3}).

The average concentrations of OC doubled in dry season (7.02±5.19 μgC m^{-3}) comparing to those in wet season (3.38±1.93 μgC m^{-3}), leading to elevated OC/EC ratio in dry season (2.56±0.94) in contrast to wet season (1.78±0.83). The hourly $AAE_{470\text{-}660}$ ranged from 1.14 to 1.67 and 1.07 to 1.76 in wet and dry seasons, respectively. As shown Figure S6a, $AAE_{470\text{-}660}$ observed in dry season (1.46±0.12) was significantly ($P<0.001$) higher than that in wet season (1.37±0.10).

Measured MAE_{520} in dry season (18.47±5.49 m^2 g^{-1}) is significantly ($P<0.001$) higher than that in wet season (10.73±4.96 m^2 g^{-1}), as shown in Figure S6b. The elevated MAE during dry season was likely a result of BB influences, which will be discussed in detail in section 3.2. The dependence of MAE_{520} on wind speed and wind direction was investigated in Figure S7, which is generated using ZeFir (Petit et al., 2017). In wet season, the southeast wind dominates (Figure S7b), which is in consistency with back-trajectory analysis discussed above. MAE_{520} did not show obvious dependence on wind speed and wind direction in the wet season (Figure S7a). In dry season, the northwestern wind prevailed (Figure S7d). High MAE_{520} was spotted from west with a wind speed at 7 m s^{-1} (Figure s7c), suggesting regional transport of aged air masses.

The MAE_{p520} values determined by MRS were 8.6 and 16.8 m^2g^{-1}, for wet and dry seasons, respectively (Figure 2a & b). Similar to MAE_{520}, the increase of MAE_{p520} in the dry season was also likely a result of BB influence, which could lead to larger BC cores (Ditas et al., 2018) and with thicker primary coatings (Schwarz et al., 2008a; Kondo et al., 2011; Lack et al., 2012a; Liu et al., 2014). More details of the BB influences will be discussed in section 3.2. Consequently, light absorption enhancement was found to be more pronounced in wet season (E_{abs520}=1.51±0.50, Table 2) than in dry season (1.29±0.28), because E_{abs} depends on the ratio of MAE to MAE_p, not their absolute values. The E_{abs} determined around the world shown diverse results (Table 2). Low E_{abs} were found in California (1.06@532 nm)(Cappa et al., 2012) and Japan (1.06@532 nm) (Ueda et al., 2016). Liu et al. (2017a) observed a moderate E_{abs} in UK (1.0-1.3@532 nm) and suggested that the small E_{abs} observed by Cappa et al. (2012) was a result of mixing state diversity. A recent study in California (Cappa et al., 2019) found moderate E_{abs} at Fresno (1.22@532 nm) but low E_{abs} at Fontana

https://doi.org/10.5194/acp-2019-654
Preprint. Discussion started: 4 November 2019


Atmospheric Chemistry and Physics Discussions

(1.07@532 nm), which was partially associated with unequal distribution of coating between different BC-containing particle types (Lee et al., 2019). In general, higher E_{abs} values had been observed in more polluted urban areas, such as France (Paris, 1.53@880 nm) (Zhang et al., 2018a), India (Kanpur, 1.8@781 nm)(Thamban et al., 2017) and various locations in China (Wang et al., 2014; Xu et al., 2016; Zhang et al., 2018b; Lan et al., 2013; Wu et al., 2018; Cui et al., 2016b; Chen et al., 2017; Bai et al., 2018; Xie et al., 2019).

Dependence of E_{abs520} on air masses was investigated by back-trajectory cluster analysis as shown in Figure S5. In wet season, the highest E_{abs520} (1.71± 0.58) was found from the shortest back trajectories (C1), suggesting the local episodic events. The high E_{abs520} from C1 (northeasterly air mass) was also confirmed by the wind rose plot (Figure S8). The elevated E_{abs520} of C1 was likely associated with high SOC/OC ratios from Aug 18 to 23 as shown by the time series plot in Figure S4a.The two oceanic air mass clusters (C2 and C3) exhibit deviated E_{abs520} characteristics. C3 represents more aged oceanic airs masses as evidenced by the lower EC (1.56 ± 0.67) and higher E_{abs520} (1.58 ± 0.57). In contrast, C2 has relatively lower E_{abs520} (1.40 ± 0.38) but higher EC. In dry season, E_{abs520} did not show clear dependence on back trajectory clusters as the E_{abs520} falls into a narrow range (1.24-1.34) between C1-C3. E_{abs} dependence on wind speed and wind direction was examined in Figure S8. E_{abs520} showed little dependence on wind speed and the high E_{abs} occurrences (Figure S8) was largely overlapped with the high MAE as shown in Figure S7.

In summary, as evidenced by $AAE_{470\text{-}660}$ and MAE results, carbonaceous aerosols exhibit a strong seasonality in urban Guanghzou. This seasonality was associated with two seasonal factors, including contrasted direction of the prevailing wind, and diverse primary BC optical properties induced by seasonal BB influence.

3.2 Influence of biomass burning on the BC optical properties during dry season

Evidence from particle chemical compositions showed that BB influence was more intense in the dry season. Levoglucosan had been widely accepted as the tracer for BB in the $PM_{2.5}$ (Engling et al., 2006; Bhattarai et al., 2019). As shown in Figure S9, levoglucosan concentrations in Guangzhou were elevated by one order of magnitude during the dry season (159.33 ng m^{-3}) comparing to those in the wet season (35.93 ng m^{-3}). Besides levoglucosan, primary OC/EC ratio can also be used as an indicator of BB influence since the BB influence samples has a higher OC/EC ratio than that from traffic emissions (Schmidl et al., 2008; Pokhrel et al., 2016). In this study, $(OC/EC)_{pri}$ determined by MRS in dry season (2.31) was higher than that in wet season (1.49), as shown in Figure S10. In addition, the northeasterly wind prevailed during the dry season, which favors long-range transport of aerosols from BB from central and eastern China to the PRD region. Remote sensing

https://doi.org/10.5194/acp-2019-654
Preprint. Discussion started: 4 November 2019


Atmospheric Chemistry and Physics Discussions

results also confirmed the more intense BB in dry season, as shown by gridded fire count map (Figure S11) determined by VIIRS.

As a result, the optical properties of BC were largely affected by the intense BB influences during the dry season. First, as shown in Figure S6b, significantly ($P<0.001$) higher MAE_{520} was observed in dry season (18.47±5.49) comparing to that in wet season (11.28±9.88). A previous field study at a suburban site in Guanghzou also reported the influence of BB on MAE, which observed a positive correlation between K^+ and MAE (Wu et al., 2018). High MAE from BB had been reported in BB emission studies as well (Roden et al., 2006; Schmidl et al., 2008; Levin et al., 2010; Wang et al., 2018a). Single particle soot photometer (SP2) studies have shown that BB influenced BC particles are more likely to have larger BC cores (Ditas et al., 2018), and with thicker initial coatings than those from vehicular emissions (Schwarz et al., 2008a; Kondo et al., 2011; Lack et al., 2012a; Liu et al., 2014). This is in good agreement with the MAE_{p520} obtained in the present study, which was almost doubled in dry season (16.8 m^2g^{-1}) comparing to that in wet season (8.6 m^2g^{-1}).

In dry season the E_{abs} showed little wavelength dependence (Figure 2d) despite the influence from BB. In this sense, the BB influence did substantially alter the optical properties of primary BC in the dry season, but the contribution of secondary BrC on E_{abs} was likely limited. The weak wavelength dependence of E_{abs} was also observed a previous study at a suburban site in Guanghzou (Wu et al., 2018). A previous study in Guangzhou also found that the seasonal difference of BrC light absorption contribution at 405 nm between dry season (15-19%) and wet seasons (12-15%) was small (Li et al., 2018d). In addition, the small seasonal difference of AAE between wet (1.37±0.10) and dry (1.46±0.12) seasons observed in this study also implies that secondary BrC contribution was not the dominating driver for AAE deviation from 1, which was the typical AAE for fresh soot without atmospheric aging. The results found in PRD were in contrast to a study in Paris, which found systematic higher E_{abs370} than E_{abs880} at wintertime due to the influence of biomass burning (Zhang et al., 2018a).This discrepancy implies the complex linkage between BB and BrC optical properties.

The complex relationship between AAE and BrC can be affected by a variety of factors. First, the optical properties of primary BrC from BB exhibit large diversity in previous studies (Martinsson et al., 2015; Tian et al., 2019a) , which can be affected by fuel type and combustion conditions (Reid et al., 2005; Roden et al., 2006). Second, atmospheric aging can lead to AAE elevation through the formation of secondary BrC from a variety of pathways (Moise et al., 2015; Laskin et al., 2015), including nitration of aromatic compounds (Jacobson, 1999), reaction of ammonia (Bones et al., 2010), bond-forming reactions between SOA

https://doi.org/10.5194/acp-2019-654
Preprint. Discussion started: 4 November 2019


Atmospheric Chemistry and Physics Discussions

constituents (Shapiro et al., 2009), reactions of biomass burning products (Gilardoni et al., 2016; Kumar et al., 2018), photo-enhancement (Hems and Abbatt, 2018; Liu et al., 2016b; Ye et al., 2019), and aqueous-phase reactions (Lin et al., 2015; Tang et al., 2016; Xu et al., 2018a).On the other hand, AAE decrease could also occur during atmospheric aging (Romonosky et al., 2019), either induced by photo-bleaching of BrC (Adler et al., 2011; Zhong and Jang, 2011, 2014; Lee et al., 2014; Canonaco et al., 2015; Lin et al., 2016; Sumlin et al., 2017; Bhattarai et al., 2018; Fortenberry et al., 2018; Hems and Abbatt, 2018; Browne et al., 2019; Dasari et al., 2019; Li et al., 2019a; Wong et al., 2019), or aqueous-phase BrC degradation in the absence of light (Santos and Duarte, 2015; Santos et al., 2016b; Santos et al., 2016a; Fan et al., 2019). The relative contribution of secondary BrC formation and BrC degradation on the total BrC light absorption budget is still poorly understood. BrC degradation could be one of the reasons of the small seasonal AAE difference observed in the PRD region. More studies are needed by incorporating both time-resolved optical measurements and time-resolved detailed chemical speciation measurements to better understand the balance of BrC formation and degradation.

3.3 Diurnal dynamics of carbonaceous aerosols concentrations and optical properties

The diurnal variations of EC, OC, OC/EC, SOC, $AAE_{470\text{-}660}$ and E_{abs520} in wet and dry seasons are shown in Figure 3. Two peaks can be observed for EC (Figure 3a), one in the early morning (7:00) and the other in the evening (19:00), which reflects local traffic emissions in two rush hours. The lowest EC was found in the afternoon (14:00), likely associated with two factors considering the nature of EC source exclusive from primary emissions. The first factor is planetary boundary layer (PBL) height. As shown in Figure S12, the diurnal maximum PBL height was at 14:00 and 15:00 for wet and dry seasons, respectively. The fully developed PBL would help dilute the concentrations of primary pollutants (Deng et al., 2016; Liu et al., 2019a; Williams et al., 2019). The second factor is the diurnal variations of traffic volume. Previous studies (Yao et al., 2013; Xie et al., 2003) showed that traffic volume during 12:00 – 15:00 is lower than those in the morning and evening rush hours. The combination of these two factors leads to the reduced EC concentrations in the afternoon. The diurnal pattern of EC is similar between wet and dry seasons, but the magnitude was greatly elevated in the dry season.

OC exhibits a bimodal distribution (Figure 3b), peaking at 13:00 and 19:00, respectively. OC can be both primary and secondary, making its diurnal pattern different from that of EC. OC/EC also has two peaks as shown in Figure 3c. The first peak appeared at 13:00 and the second peak showed up at 17:00. It is worth noting that in wet season the afternoon OC/EC peak was higher than that in the evening OC/EC peak, while in dry season the reverse is true.

https://doi.org/10.5194/acp-2019-654
Preprint. Discussion started: 4 November 2019


Atmospheric Chemistry and Physics Discussions

As shown in Figure 3d, two SOC peaks are observed in wet season, with the first SOC peak at 13:00 and the second SOC peak at 19:00. While in dry season the afternoon SOC peak was merged into the broadened evening peak. Despite the higher SOC concentrations observed in dry season, SOC formation was more active during the wet season as evidenced by the diurnal SOC/OC ratios (Figure S13a). The diurnal SOC/OC in wet season was always higher than that in dry season. It is worth noting that in wet season, despite that the SOC evening peak was comparable to the afternoon peak as shown in Figure 3d, the SOC/OC evening peak was smaller than the afternoon peak (Figure S13a). This observation implies that the SOC evening peak in the wet season was a result of the combination of pollutant accumulation (e.g. PBL decrease after sunset) and SOC formation, rather than the formation process alone. The small evening peak of SOC/OC in summer (19:00-21:00) would also be likely a result of condensation of semi-volatile organic compound (Warren et al., 2009; Pathak et al., 2008; Liang et al., 1997) due to the temperature decrease after sunset.

SOC/OC dependence on RH was investigated (Figure S13) to explore the effect of aqueous-phase secondary organic aerosol formation. During wet season, SOC/OC decreases as RH increases and the results were the same for both daytime and nighttime (Figure S13a&b). During nighttime when no solar radiation was supplied, higher RH leads to a lower SOC/OC (Figure S13b). This piece of evidence suggests that aqueous-phase reactions were unlikely the dominating pathway for SOC formation during the wet season. In dry season, SOC/OC did not show clear dependence on RH, suggesting that SOC formation is not sensitive to RH in dry season.

The diurnal trend of $AAE_{470\text{-}660}$ was similar between wet and dry seasons, which is higher in the evening and lower during the midday, but the magnitude of $AAE_{470\text{-}660}$ slightly increased during the dry season. The E_{abs520} exhibit different diurnal patterns between the wet and dry seasons. As shown in Figure 4, elevated E_{abs520} was found during nighttime in wet season but in dry season inflated E_{abs520} was observed in the afternoon. In addition, the degree of light absorption enhancement was more pronounced in the wet season. The influencing factors of dynamics are discussed in the following sections.

3.4 The diurnal correlations between AAE, *k* and E_{abs}

The loading effect correction factor used in AE33, *k*, has been found to be a useful indicator for the light absorption enhancement of BC (Drinovec et al., 2017). As shown in Figure 4a, in wet season a good anti-correlation was found between k_3 (*k* value for 520 nm) and E_{abs520} with a R^2 of 0.74. In dry season, such anti-correlation was substantially weakened ($R^2 = 0.20$) as shown in Figure 4b, likely due to the influence of BB. These results agree well with the findings reported by Drinovec et al. (2017) that *k* can be used as a BC particle coating indicator without the influence of BB. As shown in Figure 4a, a good correlation was found

https://doi.org/10.5194/acp-2019-654
Preprint. Discussion started: 4 November 2019


Atmospheric Chemistry and Physics Discussions

between $AAE_{470\text{-}660}$ with E_{abs520} (R^2=0.71). Considering the weak BB influence in wet season as discussed in section 3.2, atmospheric aging induced coating on BC particles was more likely the dominating driver of $AAE_{470\text{-}660}$ dynamics during the wet season in the PRD region. The presence of coating of BC could also explained that despite the BB influence is small in wet season, the observed average AAE (1.37±0.10) was significantly higher than the AAE of fresh BC (~1). This result is also consistent with previous studies that found non-light-absorbing coating can lead to elevated AAE up to 1.5 (Lack and Cappa, 2010; Lack and Langridge, 2013). In dry season, the variability of AAE was governed by both coating thickness and BB influence, thus leading to a degraded R^2 (0.22) between $AAE_{470\text{-}660}$ and E_{abs520} as shown in Figure 4b. A recent study showed that the diurnal pattern of BrC was moderately correlated with a BB tracer K^+ in the PRD region during the dry season (Li et al., 2019b), implying that BB did have considerable influence on AAE viability during dry season.

The spectral fingerprints of *k* were shown in Figure S14. Observations in Europe showed that the presence of BrC could lead to increased *k* at longer wavelengths (Drinovec et al., 2017). Our observations showed that the seasonal difference in spectral fingerprints of *k* between wet and dry seasons is small. Considering the limited increase of AAE in dry season and similarity of seasonal spectral fingerprints of *k*, these results suggest that, in the PRD region, despite the BB influence in dry season effectively altered the optical properties of BC aerosols, there was likely limited secondary BrC contribution on E_{abs} during the dry season, which is in agreement with discussions in section 3.2.

3.5 The influence of secondary processing on E_{abs} diurnal dynamic

Photochemical reactions play an important role in the aging process of black carbon, leading to the modification of BC morphology and optical properties as evidenced by laboratory studies (Saathoff et al., 2003; Schnaiter et al., 2005; Martinsson et al., 2015; Pei et al., 2018) and quasi-atmospheric chamber studies (Peng et al., 2017; Peng et al., 2016). Filed studies at various locations have also showed that photochemical processing can promote the light absorption enhancement of BC, including in Beijing (Liu et al., 2019b), Yangtze River Delta (Xu et al., 2018c), Xi'an (Wang et al., 2017c), Los Angels (Krasowsky et al., 2016) and Toronto (Knox et al., 2009). The concentration of odd oxygen ($O_x = O_3+NO_2$) proposed by Liu (1977) and (Levy II et al., 1985) have been widely used as the indicator of photochemical aging. In this study, the diurnal correlations between O_x and E_{abs520} were investigated to explore the effect of photochemical processing. As shown in Figure 5a, in wet season O_x and E_{abs520} peaked at 15:00 and 0:00, respectively. The O_x experienced a continuous decline since 15:00 until the sunrise of the next day, but the growth of E_{abs} extended to midnight. The nighttime E_{abs520} peak suggests that the increase of coating can be achieved without the presence of solar

https://doi.org/10.5194/acp-2019-654
Preprint. Discussion started: 4 November 2019


Atmospheric Chemistry and Physics Discussions

radiation. These differences in the diurnal patterns led to a low correlation between O_x and E_{abs} (R^2=0.01). This result implies that in wet season the diurnal variability of E_{abs520} was unlikely dominated by photochemical reactions, despite that O_x was more pronounced in the wet season. As for dry season (Figure 5b), both O_x and E_{abs520} peaked at 17:00 leading to a good correlation with a R^2 of 0.69, suggesting that photochemical reactions could be one of the main drivers for E_{abs} diurnal variations. This result strongly indicates that BC light absorption can be markedly amplified through photochemical reactions. Our dry-season results are consistent with a previous study in Northern China (Wang et al., 2017c), which also showed the dependence of light absorption enhancement on O_x during the wintertime.

In the meantime, the formation of SOC also contributes to light absorption enhancement of BC, which had been observed in both field studies (Moffet and Prather, 2009; Wang et al., 2017a; Zhang et al., 2018a) and laboratory studies (Schnaiter et al., 2005; Lambe et al., 2013; Saliba et al., 2016). In this study, the effect of SOC formation on E_{abs} was investigated using SOC/OC as the indicator rather than using SOC alone. The advantage of using SOC/OC is that the SOC variations induced by non-secondary-formation process (e.g. PBLH shallowing) can be minimized, thereby focusing the analysis on the effect of secondary formation processes. A good diurnal correlation between SOC/OC and E_{abs520} were observed in dry season (R^2=0.53), but no correlation was found in wet season (R^2=0.01). The E_{abs} dependence on SOC/OC was examined in Figure 6. E_{abs} dependence on SOC/OC was found in both wet and dry seasons, but a clearer dependence was observed in the dry season. The results from Figure 6 suggest that the poor diurnal correlation between SOC/OC and E_{abs520} observed in wet season (Figure 5a) does not necessarily rule out the contribution of SOC on E_{abs520}. A study in Paris (Zhang et al., 2018a) found that more oxidized oxygenated organic aerosols (MOOOA) and less oxidized OOA (LO-OOA), which are surrogates of SOA, were the dominating contributors for E_{abs}, especially in summertime. In the present study, due to the lack of quantitative chemical speciation data, quantification of contributions from different chemical species on E_{abs} is not possible. A recent study in Guangzhou (Wu et al., 2019) found that traffic-derived SOC could be a significant source of SOC in the urban area, which can account for half of the total SOC. In that sense, traffic emissions are expected to have a considerable contribution to BC light absorption enhancement in both wet and dry seasons.

3.6 The influence of semi-volatile compounds on E_{abs} diurnal variations

The SPAMS data from both wet (August 11-18, 2017) and dry season (15 November 2017 to 27 December 2017) were analyzed to explore the mixing state of EC-containing particles from a single-particle perspective. The average EC-fresh and EC-aged mass spectra are shown in Figure S15 for both wet and dry seasons. The domination of EC-aged particles in EC-containing particles number fraction suggest that most of the EC

https://doi.org/10.5194/acp-2019-654
Preprint. Discussion started: 4 November 2019


Atmospheric Chemistry and Physics Discussions

particles are internally mixed with other species (Table S2). This result agrees with previous studies in this region (Zhang et al., 2013; Zhang et al., 2014).

To study the relative abundance of coating materials on EC particles, we investigate the ratios of RPA by different species (organics, sulfate and nitrate) to RPA by EC in both wet and dry seasons (Figure 7). In wet season, organics and sulfate on EC-containing particles demonstrated similar diurnal trends that both peaked at 13:00, implying the association with photochemical reactions. The timing of the organic peak by SPAMS shown in Figure 7a also agrees well with the bulk measurements of SOC/OC (Figure 5a). However, the diurnal variations of organics and sulfate were poorly correlated with E_{abs520} as shown by the low R^2 in the scatter plot in Figure 7a&b. It should be noted that poor diurnal correlations do not necessarily rule out the contribution of organics and sulfate to E_{abs} by analogy with the SOC correlation with E_{abs} as discussed in section 3.5. Although the quantitative contribution estimation of sulfate and SOA to E_{abs} is not possible in this study, a rough estimation can be projected. Considering the typical annual average SOC concentration (3 μgC m^{-3})(Wu et al., 2019), typical SOA/SOC mass ratio (1.8) (Li et al., 2017), and sulfate concentration (8 μg m^{-3})(Liu et al., 2017b) in the PRD region, SOA and sulfate would likely have comparable contributions to the $E_{abs,}$ according to the E_{abs} dependency on sulfate-to-SOA mass ratio results by Zhang et al. (2018a). Summertime nitrate was low in daytime and high in nighttime (Figure 7c), which agrees with measurements at the roadside site in Hong Kong (Lee et al., 2015) and Shanghai (Li et al., 2018b). Temperature-dependent gas-particle partitioning would be one of the possible reasons for the observed nitrate diurnal pattern (Appel et al., 1981; Xue et al., 2014; Griffith et al., 2015). Higher temperature during the daytime (Figure S16) favors HNO_3 partitioning into the gas-phase in wet season. The diurnal pattern of nitrate correlates well with that of E_{abs520} (R^2=0.59) as shown in Figure 7c, suggesting that E_{abs520} was likely affected by temperature-induced gas-particle partitioning during wet season. A previous chamber study had shown the decrease of E_{abs} due to SOA evaporation (Metcalf et al., 2013). By analogy with nitrate, organic compounds with a volatility similar to nitrate might potentially involve in shaping the diurnal pattern of E_{abs} in wet season.

In dry season, organics were moderately correlated with E_{abs520} (R^2=0.38) as shown in Figure 7d. The improved correlation of organics in dry season was in agreement with O_x and SOC/OC results as shown in Figure 5b. Sulfate was still poorly correlated with E_{abs520}. Since the contribution of sulfate on E_{abs520} cannot be ruled out, one possible explanation is that the contribution of sulfate on E_{abs520} was not reflected on the diurnal time scale.

5. Conclusions and implications

This study explored the temporal dynamics of optical properties of carbonaceous aerosols in urban

https://doi.org/10.5194/acp-2019-654
Preprint. Discussion started: 4 November 2019

Atmospheric Chemistry and Physics Discussions

Guangzhou, a typical megacity in southern China, focusing on the atmospheric aging induced light absorption enhancement of BC. Field measurements were conducted at an urban site during wet season (July 31–September 10, 2017) and dry season (November 15, 2017–January 15, 2018). A newly developed approach, the minimum R squared (MRS) method (Wu et al., 2018), was applied to determine the light absorption enhancement factor, E_{abs}, using data from a Aethalometer and a field-deployable semi-continuous carbon analyzer. The MRS approach avoids specialized instrument setup (e.g. thermal denuder and photo-acoustic spectrometer) for E_{abs} determination, hence has a great potential for expending data pool of E_{abs}, considering the fact that collocated Aethalometer and field carbon analyzer measurements have been widely deployed around the world.

A strong seasonality of BC was observed. The average concentration of EC was 1.94±0.93 and 2.81±2.01 μgC m^{-3} in the wet and dry seasons, respectively. Collective evidence from remote sensing fire counts and ground measurements of levoglucosan showed that biomass burning (BB) was more active in the dry season. Consequently, optical properties of BC were effectively altered, leading to elevated MAE (dry season: 18.47±5.49 m^2 g^{-1}, wet season: 10.73±4.96 m^2 g^{-1}), MAE_p (dry season: 15.8 m^2 g^{-1}, wet season: 8.1 m^2 g^{-1}) and AAE (dry season: 1.46±0.12, wet season: 1.37±0.10) in dry season comparing to those in wet season. However, little dependence of E_{abs} on wavelength was observed in dry season despite the influence from BB. The diurnal correlation analysis between AAE, *k* and E_{abs} revealed different results between wet and dry seasons. During the wet season when BB influence was small, AAE was well correlated with E_{abs}, implying that coating was likely the main driver for AAE>1. In other words, the two component AAE model might not be suitable for BrC absorption estimation under such circumstance. The aethalometer loading effect correction factor, *k*, was confirmed to be a useful E_{abs} indicator owing to its good correlation with E_{abs} during the wet season. In dry season, the weak correlation between AAE and E_{abs} implies the contribution from BB on AAE. In dry season, the BB influence leads to poor correlation between *k* and E_{abs}, confirming that *k* can only be used as the coating indicator when BB influence is small.

The effect of atmospheric aging on E_{abs} diurnal pattern was examined. O_x and SOC/OC were found well correlated with E_{abs} during the dry season but no correlation was observed in the wet season. However, further analysis showed E_{abs} dependence on SOC/OC in both wet and dry season. This observation implies that poor diurnal correlation in wet season does not necessarily rule out the E_{abs} contribution from SOC. In other words, the SOC contribution on E_{abs} in wet season was not necessarily be reflected in mere diurnal correlation. A good diurnal correlation between nitrate and E_{abs} was observed, implying the potential role of semi-volatile components in regulating the diurnal dynamics of E_{abs}. In China, the sulfate problem had been effectively

https://doi.org/10.5194/acp-2019-654
Preprint. Discussion started: 4 November 2019

mitigated by the reduction measures implemented in recent years (Xia et al., 2016; Wang et al., 2017b). In contrast, nitrate increased substantially in the recent years (Xu et al., 2019; Tian et al., 2019b). As a result, the increasing nitrate might potentially affect BC's radiative forcing in China.

https://doi.org/10.5194/acp-2019-654
Preprint. Discussion started: 4 November 2019

Atmospheric Chemistry and Physics Discussions

Appendix

Table A1. Abbreviations.

Abbreviation	Definition
$AAE_{470–660}$	Ångström absorption exponent between 470 and 660 nm
AFD	aerosol filter filtration-dissolution
BB	biomass burning
BC	black carbon
BrC	brown carbon
E_{abs520}	light absorption enhancement factor at 520 nm
σ_{abs520}	light absorption coefficient at 520 nm
σ_{abs_total}	total light absorption coefficient of a coated particle
σ_{abs_pri}	primary light absorption coefficient attributed to the soot core alone of a coated particle
σ_{abs_aging}	extra light absorption other than σ_{abs_pri}, including those from the lensing effect arise from non-absorbing coating on the soot core and secondary brown carbon during atmospheric aging
eBC	equivalent BC mass concentration determined by optical methods (e.g. aethalometer)
$k_1, k_2 \ldots k_7$	compensation factors (Eqs. 5 & 6) at 7 wavelengths (370,470,520,590,660, 880 and 950 nm).
MAE_{520}	mass absorption efficiency at 520 nm, also known as mass absorption cross section (MAC)
MAE_p	primary MAE of freshly emitted soot particles
MAE_{p_h}	a series of hypothetical MAE_p tested in MRS calculation
MRS	minimum R squared method
OC	organic carbon
PRD	Pearl River Delta region, China
rBC	refectory black carbon (commonly used for reporting BC detected by SP2)
r_{aged}	The ratio of aged particles to fresh particles determined by SP2
SP2	single-particle soot photometer
SSA	single-scattering albedo
TD	thermodenuder

https://doi.org/10.5194/acp-2019-654
Preprint. Discussion started: 4 November 2019

Author contributions

C.W. designed the study. J.Y.S. and C.W. performed the experiments. J.Y.S., C.W., C.C., Q.Z. and Y.L. conducted the data analysis. J.Y.S. and C.W. wrote the paper with the inputs from all authors.

Data availability

OC, EC, and σ_{abs} data used in this study are available from corresponding authors upon request.

Competing interests

The authors declare that they have no conflict of interest.

Acknowledgements

This work is supported by the National Key Research and Development Program of China (grant No. 2016YFC0208503), National Natural Science Foundation of China (grant No.41605002, 41475004), Guangzhou Science and Technology Project (grant No.201604016053), Major Project of Industry-University-Research Collaborative Innovation in Guangzhou (grant No.2016201604030082) and Pearl River Nova Program of Guangzhou (grant No.201610010149). The authors gratefully acknowledge the NOAA Air Resources Laboratory (ARL) for the provision of the HYSPLIT transport and dispersion model used in this publication. We acknowledge the use of data from the NASA FIRMS application (https://firms.modaps.eosdis.nasa.gov/) operated by the NASA/Goddard Space Flight Center Earth Science Data and Information System (ESDIS) project.

https://doi.org/10.5194/acp-2019-654
Preprint. Discussion started: 4 November 2019

Atmospheric Chemistry and Physics Discussions

References

Adler, G., Riziq, A. A., Erlick, C., and Rudich, Y.: Effect of intrinsic organic carbon on the optical properties of fresh diesel soot, Proceedings of the National Academy of Sciences, 107, 6699-6704, doi: 10.1073/pnas.0903311106, 2010.

Adler, G., Flores, J. M., Abo Riziq, A., Borrmann, S., and Rudich, Y.: Chemical, physical, and optical evolution of biomass burning aerosols: a case study, Atmos. Chem. Phys., 11, 1491-1503, doi: 10.5194/acp-11-1491-2011, 2011.

Albrecht, B. A.: Aerosols, Cloud Microphysics, and Fractional Cloudiness, Science, 245, 1227-1230, doi: 10.1126/science.245.4923.1227, 1989.

Anderson, T. L., Charlson, R. J., Schwartz, S. E., Knutti, R., Boucher, O., Rodhe, H., and Heintzenberg, J.: Climate forcing by aerosols - a hazy picture, Science, 300, 1103-1104, doi: 10.1126/science.1084777, 2003.

Appel, B. R., Tokiwa, Y., and Haik, M.: Sampling of nitrates in ambient air, Atmos. Environ., 15, 283-289, doi: 10.1016/0004-6981(81)90029-9, 1981.

Apte, J. S., Marshall, J. D., Cohen, A. J., and Brauer, M.: Addressing Global Mortality from Ambient PM2.5, Environ. Sci. Technol., 49, 8057-8066, doi: 10.1021/acs.est.5b01236, 2015.

Bai, Z., Cui, X., Wang, X., Xie, H., and Chen, B.: Light absorption of black carbon is doubled at Mt. Tai and typical urban area in North China, Sci.Total.Environ., 635, 1144-1151, doi: 10.1016/j.scitotenv.2018.04.244, 2018.

Bambha, R. P., Dansson, M. A., Schrader, P. E., and Michelsen, H. A.: Effects of volatile coatings and coating removal mechanisms on the morphology of graphitic soot, Carbon, 61, 80-96, doi: 10.1016/j.carbon.2013.04.070, 2013.

Bhattarai, C., Samburova, V., Sengupta, D., Iaukea-Lum, M., Watts, A. C., Moosmüller, H., and Khlystov, A. Y.: Physical and chemical characterization of aerosol in fresh and aged emissions from open combustion of biomass fuels, Aerosol. Sci. Technol., 52, 1266-1282, doi: 10.1080/02786826.2018.1498585, 2018.

Bhattarai, H., Saikawa, E., Wan, X., Zhu, H., Ram, K., Gao, S., Kang, S., Zhang, Q., Zhang, Y., Wu, G., Wang, X., Kawamura, K., Fu, P., and Cong, Z.: Levoglucosan as a tracer of biomass burning: Recent progress and perspectives, Atmos Res, 220, 20-33, doi: 10.1016/j.atmosres.2019.01.004, 2019.

Bian, Q., Alharbi, B., Shareef, M. M., Husain, T., Pasha, M. J., Atwood, S. A., and Kreidenweis, S. M.: Sources of PM2.5 carbonaceous aerosol in Riyadh, Saudi Arabia, Atmos. Chem. Phys., 18, 3969-3985, doi: 10.5194/acp-18-3969-2018, 2018.

Bond, T. C. and Bergstrom, R. W.: Light absorption by carbonaceous particles: An investigative review, Aerosol. Sci. Technol., 40, 27-67, doi: 10.1080/02786820500421521, 2006.

Bond, T. C., Habib, G., and Bergstrom, R. W.: Limitations in the enhancement of visible light absorption due to mixing state, J. Geophys. Res., 111, D20211, doi: 10.1029/2006JD007315, 2006.

Bond, T. C., Doherty, S. J., Fahey, D. W., Forster, P. M., Berntsen, T., DeAngelo, B. J., Flanner, M. G., Ghan, S., Karcher, B., Koch, D., Kinne, S., Kondo, Y., Quinn, P. K., Sarofim, M. C., Schultz, M. G., Schulz, M., Venkataraman, C., Zhang, H., Zhang, S., Bellouin, N., Guttikunda, S. K., Hopke, P. K., Jacobson, M. Z., Kaiser, J. W., Klimont, Z., Lohmann, U., Schwarz, J. P., Shindell, D., Storelvmo, T., Warren, S. G., and Zender, C. S.: Bounding the role of black carbon in the climate system: A scientific assessment, J. Geophys. Res., 118, 5380-5552, doi: 10.1002/jgrd.50171, 2013.

Bones, D. L., Henricksen, D. K., Mang, S. A., Gonsior, M., Bateman, A. P., Nguyen, T. B., Cooper, W. J., and Nizkorodov, S. A.: Appearance of strong absorbers and fluorophores in limonene-O3 secondary organic aerosol due to NH4+-mediated chemical aging over long time scales, J. Geophys. Res., 115, doi: 10.1029/2009jd012864, 2010.

Browne, E. C., Zhang, X., Franklin, J. P., Ridley, K. J., Kirchstetter, T. W., Wilson, K. R., Cappa, C. D., and Kroll, J. H.: Effect of heterogeneous oxidative aging on light absorption by biomass burning organic aerosol, Aerosol. Sci. Technol., 53, 663-674, doi: 10.1080/02786826.2019.1599321, 2019.

Burtscher, H., Baltensperger, U., Bukowiecki, N., Cohn, P., Hüglin, C., Mohr, M., Matter, U., Nyeki, S., Schmatloch, V., Streit, N., and Weingartner, E.: Separation of volatile and non-volatile aerosol fractions by thermodesorption: instrumental development and applications, J. Aerosol. Sci., 32, 427-442, doi: 10.1016/S0021-8502(00)00089-6, 2001.

Canonaco, F., Slowik, J. G., Baltensperger, U., and Prévôt, A. S. H.: Seasonal differences in oxygenated organic aerosol composition: implications for emissions sources and factor analysis, Atmos. Chem. Phys., 15, 6993-7002, doi: 10.5194/acp-15-

6993-2015, 2015.

Cappa, C. D., Onasch, T. B., Massoli, P., Worsnop, D. R., Bates, T. S., Cross, E. S., Davidovits, P., Hakala, J., Hayden, K. L., Jobson, B. T., Kolesar, K. R., Lack, D. A., Lerner, B. M., Li, S.-M., Mellon, D., Nuaaman, I., Olfert, J. S., Petäjä, T., Quinn, P. K., Song, C., Subramanian, R., Williams, E. J., and Zaveri, R. A.: Radiative Absorption Enhancements Due to the Mixing State of Atmospheric Black Carbon, Science, 337, 1078-1081, doi: 10.1126/science.1223447, 2012.

Cappa, C. D., Zhang, X., Russell, L. M., Collier, S., Lee, A. K. Y., Chen, C.-L., Betha, R., Chen, S., Liu, J., Price, D. J., Sanchez, K. J., McMeeking, G. R., Williams, L. R., Onasch, T. B., Worsnop, D. R., Abbatt, J., and Zhang, Q.: Light absorption by ambient black and brown carbon and its dependence on black carbon coating state for two California, USA cities in winter and summer, J. Geophys. Res., 124, 1550-1577, doi: 10.1029/2018JD029501, 2019.

Chen, B., Bai, Z., Cui, X., Chen, J., Andersson, A., and Gustafsson, Ö.: Light absorption enhancement of black carbon from urban haze in Northern China winter, Environ. Pollut., 221, 418-426, doi: 10.1016/j.envpol.2016.12.004, 2017.

Chen, H., Hu, D., Wang, L., Mellouki, A., and Chen, J.: Modification in light absorption cross section of laboratory-generated black carbon-brown carbon particles upon surface reaction and hydration, Atmos. Environ., 116, 253-261, doi: 10.1016/j.atmosenv.2015.06.052, 2015.

Cheng, Y., Engling, G., Moosmüller, H., Arnott, W. P., Chen, L. W. A., Wold, C. E., Hao, W. M., and He, K.-b.: Light absorption by biomass burning source emissions, Atmos. Environ., 127, 347-354, doi: 10.1016/j.atmosenv.2015.12.045, 2016.

Chung, S. H. and Seinfeld, J. H.: Global distribution and climate forcing of carbonaceous aerosols, J. Geophys. Res., 107, doi: 10.1029/2001JD001397, 2002.

Conrad, B. M. and Johnson, M. R.: Mass absorption cross-section of flare-generated black carbon: Variability, predictive model, and implications, Carbon, doi: 10.1016/j.carbon.2019.04.086, 2019.

Csiszar, I., Schroeder, W., Giglio, L., Ellicott, E., Vadrevu, K. P., Justice, C. O., and Wind, B.: Active fires from the Suomi NPP Visible Infrared Imaging Radiometer Suite: Product status and first evaluation results, J. Geophys. Res., 119, 803-816, doi: 10.1002/2013jd020453, 2014.

Cui, F., Chen, M., Ma, Y., Zheng, J., Zhou, Y., Li, S., Qi, L., and Wang, L.: An intensive study on aerosol optical properties and affecting factors in Nanjing, China, Journal of Environmental Sciences, 40, 35-43, doi: 10.1016/j.jes.2015.08.017, 2016a.

Cui, X., Wang, X., Yang, L., Chen, B., Chen, J., Andersson, A., and Gustafsson, Ö.: Radiative absorption enhancement from coatings on black carbon aerosols, Sci.Total.Environ., 551, 51-56, doi: 10.1016/j.scitotenv.2016.02.026, 2016b.

Dasari, S., Andersson, A., Bikkina, S., Holmstrand, H., Budhavant, K., Satheesh, S., Asmi, E., Kesti, J., Backman, J., Salam, A., Bisht, D. S., Tiwari, S., Hameed, Z., and Gustafsson, Ö.: Photochemical degradation affects the light absorption of water-soluble brown carbon in the South Asian outflow, Science Advances, 5, eaau8066, doi: 10.1126/sciadv.aau8066, 2019.

Dastanpour, R., Momenimovahed, A., Thomson, K., Olfert, J., and Rogak, S.: Variation of the optical properties of soot as a function of particle mass, Carbon, 124, 201-211, doi: 10.1016/j.carbon.2017.07.005, 2017.

Deng, T., Deng, X., Li, F., Wang, S., and Wang, G.: Study on aerosol optical properties and radiative effect in cloudy weather in the Guangzhou region, Sci.Total.Environ., 568, 147-154, doi: 10.1016/j.scitotenv.2016.05.156, 2016.

Ding, A. J., Huang, X., Nie, W., Sun, J. N., Kerminen, V. M., Petäjä, T., Su, H., Cheng, Y. F., Yang, X. Q., Wang, M. H., Chi, X. G., Wang, J. P., Virkkula, A., Guo, W. D., Yuan, J., Wang, S. Y., Zhang, R. J., Wu, Y. F., Song, Y., Zhu, T., Zilitinkevich, S., Kulmala, M., and Fu, C. B.: Enhanced haze pollution by black carbon in megacities in China, Geophys. Res. Lett., 43, 2873-2879, doi: 10.1002/2016GL067745, 2016.

Ditas, J., Ma, N., Zhang, Y., Assmann, D., Neumaier, M., Riede, H., Karu, E., Williams, J., Scharffe, D., Wang, Q., Saturno, J., Schwarz, J. P., Katich, J. M., McMeeking, G. R., Zahn, A., Hermann, M., Brenninkmeijer, C. A. M., Andreae, M. O., Pöschl, U., Su, H., and Cheng, Y.: Strong impact of wildfires on the abundance and aging of black carbon in the lowermost stratosphere, Proceedings of the National Academy of Sciences, 115, E11595-E11603, doi: 10.1073/pnas.1806868115, 2018.

Draxier, R. R. and Hess, G. D.: An overview of the HYSPLIT_4 modelling system for trajectories, dispersion and deposition, Aust Meteorol Mag, 47, 295-308, 1998.

Drinovec, L., Močnik, G., Zotter, P., Prévôt, A. S. H., Ruckstuhl, C., Coz, E., Rupakheti, M., Sciare, J., Müller, T., Wiedensohler, A., and Hansen, A. D. A.: The "dual-spot" Aethalometer: an improved measurement of aerosol black carbon with real-time loading

https://doi.org/10.5194/acp-2019-654
Preprint. Discussion started: 4 November 2019

compensation, Atmos. Meas. Tech., 8, 1965-1979, doi: 10.5194/amt-8-1965-2015, 2015.

Drinovec, L., Gregorič, A., Zotter, P., Wolf, R., Bruns, E. A., Prévôt, A. S. H., Petit, J. E., Favez, O., Sciare, J., Arnold, I. J., Chakrabarty, R. K., Moosmüller, H., Filep, A., and Močnik, G.: The filter-loading effect by ambient aerosols in filter absorption photometers depends on the coating of the sampled particles, Atmos. Meas. Tech., 10, 1043-1059, doi: 10.5194/amt-10-1043-2017, 2017.

Engling, G., Carrico, C. M., Kreidenweis, S. M., Collett Jr, J. L., Day, D. E., Malm, W. C., Lincoln, E., Min Hao, W., Iinuma, Y., and Herrmann, H.: Determination of levoglucosan in biomass combustion aerosol by high-performance anion-exchange chromatography with pulsed amperometric detection, Atmos. Environ., 40, Supplement 2, 299-311, doi: 10.1016/j.atmosenv.2005.12.069, 2006.

Fan, X., Yu, X., Wang, Y., Xiao, X., Li, F., Xie, Y., Wei, S., Song, J., and Peng, P. a.: The aging behaviors of chromophoric biomass burning brown carbon during dark aqueous hydroxyl radical oxidation processes in laboratory studies, Atmos. Environ., 205, 9-18, doi: 10.1016/j.atmosenv.2019.02.039, 2019.

Fang, Y., Chen, Y., Lin, T., Hu, L., Tian, C., Luo, Y., Yang, X., Li, J., and Zhang, G.: Spatiotemporal Trends of Elemental Carbon and Char/Soot Ratios in Five Sediment Cores from Eastern China Marginal Seas: Indicators of Anthropogenic Activities and Transport Patterns, Environ. Sci. Technol., 52, 9704-9712, doi: 10.1021/acs.est.8b00033, 2018.

Fierce, L., Bond, T. C., Bauer, S. E., Mena, F., and Riemer, N.: Black carbon absorption at the global scale is affected by particle-scale diversity in composition, Nature Communications, 7, 12361, doi: 10.1038/ncomms12361, 2016.

Flanner, M. G., Zender, C. S., Randerson, J. T., and Rasch, P. J.: Present-day climate forcing and response from black carbon in snow, J. Geophys. Res., 112, doi: 10.1029/2006JD008003 2007.

Fortenberry, C. F., Walker, M. J., Zhang, Y., Mitroo, D., Brune, W. H., and Williams, B. J.: Bulk and molecular-level characterization of laboratory-aged biomass burning organic aerosol from oak leaf and heartwood fuels, Atmos. Chem. Phys., 18, 2199-2224, doi: 10.5194/acp-18-2199-2018, 2018.

Fuller, K. A., Malm, W. C., and Kreidenweis, S. M.: Effects of mixing on extinction by carbonaceous particles, J. Geophys. Res., 104, 15941-15954, doi: 10.1029/1998JD100069, 1999.

Gertler, C. G., Puppala, S. P., Panday, A., Stumm, D., and Shea, J.: Black carbon and the Himalayan cryosphere: A review, Atmos. Environ., 125, 404-417, doi: 10.1016/j.atmosenv.2015.08.078, 2016.

Ghazi, R. and Olfert, J. S.: Coating Mass Dependence of Soot Aggregate Restructuring due to Coatings of Oleic Acid and Dioctyl Sebacate, Aerosol. Sci. Technol., 47, 192-200, doi: 10.1080/02786826.2012.741273, 2013.

Gilardoni, S., Massoli, P., Paglione, M., Giulianelli, L., Carbone, C., Rinaldi, M., Decesari, S., Sandrini, S., Costabile, F., Gobbi, G. P., Pietrogrande, M. C., Visentin, M., Scotto, F., Fuzzi, S., and Facchini, M. C.: Direct observation of aqueous secondary organic aerosol from biomass-burning emissions, Proceedings of the National Academy of Sciences, 113, 10013-10018, doi: 10.1073/pnas.1602212113, 2016.

Grahame, T. J., Klemm, R., and Schlesinger, R. B.: Public health and components of particulate matter: The changing assessment of black carbon, J. Air Waste Manage. Assoc., 64, 620-660, doi: 10.1080/10962247.2014.912692, 2014.

Griffith, S. M., Huang, X. H. H., Louie, P. K. K., and Yu, J. Z.: Characterizing the thermodynamic and chemical composition factors controlling PM2.5 nitrate: Insights gained from two years of online measurements in Hong Kong, Atmos. Environ., 122, 864-875, doi: 10.1016/j.atmosenv.2015.02.009, 2015.

Gross, D. S., Gälli, M. E., Silva, P. J., and Prather, K. A.: Relative Sensitivity Factors for Alkali Metal and Ammonium Cations in Single-Particle Aerosol Time-of-Flight Mass Spectra, Anal. Chem., 72, 416-422, doi: 10.1021/ac990434g, 2000.

Hallquist, M., Wenger, J. C., Baltensperger, U., Rudich, Y., Simpson, D., Claeys, M., Dommen, J., Donahue, N. M., George, C., Goldstein, A. H., Hamilton, J. F., Herrmann, H., Hoffmann, T., Iinuma, Y., Jang, M., Jenkin, M. E., Jimenez, J. L., Kiendler-Scharr, A., Maenhaut, W., McFiggans, G., Mentel, T. F., Monod, A., Prevot, A. S. H., Seinfeld, J. H., Surratt, J. D., Szmigielski, R., and Wildt, J.: The formation, properties and impact of secondary organic aerosol: current and emerging issues, Atmos. Chem. Phys., 9, 5155-5236, doi: 10.5194/acp-9-5155-2009, 2009.

Hansen, J. and Nazarenko, L.: Soot climate forcing via snow and ice albedos, P Natl Acad Sci USA, 101, 423-428, doi: 10.1073/pnas.2237157100, 2004.

https://doi.org/10.5194/acp-2019-654
Preprint. Discussion started: 4 November 2019

Hatch, L. E., Pratt, K. A., Huffman, J. A., Jimenez, J. L., and Prather, K. A.: Impacts of Aerosol Aging on Laser Desorption/Ionization in Single-Particle Mass Spectrometers, Aerosol. Sci. Technol., 48, 1050-1058, doi: 10.1080/02786826.2014.955907, 2014.

He, C., Flanner, M. G., Chen, F., Barlage, M., Liou, K. N., Kang, S., Ming, J., and Qian, Y.: Black carbon-induced snow albedo reduction over the Tibetan Plateau: uncertainties from snow grain shape and aerosol–snow mixing state based on an updated SNICAR model, Atmos. Chem. Phys., 18, 11507-11527, doi: 10.5194/acp-18-11507-2018, 2018.

Healy, R. M., Wang, J. M., Jeong, C. H., Lee, A. K. Y., Willis, M. D., Jaroudi, E., Zimmerman, N., Hilker, N., Murphy, M., Eckhardt, S., Stohl, A., Abbatt, J. P. D., Wenger, J. C., and Evans, G. J.: Light-absorbing properties of ambient black carbon and brown carbon from fossil fuel and biomass burning sources, J. Geophys. Res., 120, 2015JD023382, doi: 10.1002/2015JD023382, 2015.

Hems, R. F. and Abbatt, J. P. D.: Aqueous Phase Photo-oxidation of Brown Carbon Nitrophenols: Reaction Kinetics, Mechanism, and Evolution of Light Absorption, ACS Earth and Space Chemistry, 2, 225-234, doi: 10.1021/acsearthspacechem.7b00123, 2018.

Huang, X. H., Bian, Q., Louie, P., and Yu, J.: Contributions of vehicular carbonaceous aerosols to PM 2.5 in a roadside environment in Hong Kong, Atmos. Chem. Phys., 14, 9279-9293, doi: 10.5194/acp-14-9279-2014, 2014.

Huntzicker, J. J., Johnson, R. L., Shah, J. J., and Cary, R. A.: Analysis of Organic and Elemental Carbon in Ambient Aerosols by a Thermal-Optical Method, in: Particulate Carbon: Atmospheric Life Cycle, edited by: Wolff, G. T., and Klimisch, R. L., Springer US, Boston, MA, 79-88, 1982.

IPCC: Climate change 2013 : the physical science basis : Working Group I contribution to the Fifth Assessment Report of the Intergovernmental Panel on Climate Change, xi, 1535 pages. pp., 2013.

Irwin, M., Kondo, Y., Moteki, N., and Miyakawa, T.: Evaluation of a Heated-Inlet for Calibration of the SP2, Aerosol. Sci. Technol., 47, 895-905, doi: 10.1080/02786826.2013.800187, 2013.

Jacobson, M. Z.: Isolating nitrated and aromatic aerosols and nitrated aromatic gases as sources of ultraviolet light absorption, J. Geophys. Res., 104, 3527-3542, doi: 10.1029/1998jd100054, 1999.

Jacobson, M. Z.: Strong radiative heating due to the mixing state of black carbon in atmospheric aerosols, Nature, 409, 695-697, doi: 10.1038/35055518, 2001.

Jeong, C. H., McGuire, M. L., Godri, K. J., Slowik, J. G., Rehbein, P. J. G., and Evans, G. J.: Quantification of aerosol chemical composition using continuous single particle measurements, Atmos. Chem. Phys., 11, 7027-7044, doi: 10.5194/acp-11-7027-2011, 2011.

Ji, D., Gao, M., Maenhaut, W., He, J., Wu, C., Cheng, L., Gao, W., Sun, Y., Sun, J., Xin, J., Wang, L., and Wang, Y.: The carbonaceous aerosol levels still remain a challenge in the Beijing-Tianjin-Hebei region of China: Insights from continuous high temporal resolution measurements in multiple cities, Environ. Int., 126, 171-183, doi: 10.1016/j.envint.2019.02.034, 2019.

Ji, Y., Qin, X., Wang, B., Xu, J., Shen, J., Chen, J., Huang, K., Deng, C., Yan, R., Xu, K., and Zhang, T.: Counteractive effects of regional transport and emission control on the formation of fine particles: a case study during the Hangzhou G20 summit, Atmos. Chem. Phys., 18, 13581-13600, doi: 10.5194/acp-18-13581-2018, 2018.

Johansson, K. O., Head-Gordon, M. P., Schrader, P. E., Wilson, K. R., and Michelsen, H. A.: Resonance-stabilized hydrocarbon-radical chain reactions may explain soot inception and growth, Science, 361, 997-1000, doi: 10.1126/science.aat3417, 2018.

Kanakidou, M., Seinfeld, J. H., Pandis, S. N., Barnes, I., Dentener, F. J., Facchini, M. C., Van Dingenen, R., Ervens, B., Nenes, A., Nielsen, C. J., Swietlicki, E., Putaud, J. P., Balkanski, Y., Fuzzi, S., Horth, J., Moortgat, G. K., Winterhalter, R., Myhre, C. E. L., Tsigaridis, K., Vignati, E., Stephanou, E. G., and Wilson, J.: Organic aerosol and global climate modelling: a review, Atmos. Chem. Phys., 5, 1053-1123, doi: 10.5194/acp-5-1053-2005, 2005.

Kaufman, Y. J. and Koren, I.: Smoke and pollution aerosol effect on cloud cover, Science, 313, 655-658, doi: 10.1126/science.1126232, 2006.

Knox, A., Evans, G. J., Brook, J. R., Yao, X., Jeong, C. H., Godri, K. J., Sabaliauskas, K., and Slowik, J. G.: Mass Absorption Cross-Section of Ambient Black Carbon Aerosol in Relation to Chemical Age, Aerosol. Sci. Technol., 43, 522-532, doi: 10.1080/02786820902777207, 2009.

Koch, D. and Del Genio, A.: Black carbon semi-direct effects on cloud cover: review and synthesis, Atmos. Chem. Phys., 10, 7685-7696, doi: 10.5194/acp-10-7685-2010, 2010.

https://doi.org/10.5194/acp-2019-654
Preprint. Discussion started: 4 November 2019

Kondo, Y., Matsui, H., Moteki, N., Sahu, L., Takegawa, N., Kajino, M., Zhao, Y., Cubison, M. J., Jimenez, J. L., Vay, S., Diskin, G. S., Anderson, B., Wisthaler, A., Mikoviny, T., Fuelberg, H. E., Blake, D. R., Huey, G., Weinheimer, A. J., Knapp, D. J., and Brune, W. H.: Emissions of black carbon, organic, and inorganic aerosols from biomass burning in North America and Asia in 2008, J. Geophys. Res., 116, D08204, doi: 10.1029/2010jd015152, 2011.

Kopacz, M., Mauzerall, D. L., Wang, J., Leibensperger, E. M., Henze, D. K., and Singh, K.: Origin and radiative forcing of black carbon transported to the Himalayas and Tibetan Plateau, Atmos. Chem. Phys., 11, 2837-2852, doi: 10.5194/acp-11-2837-2011, 2011.

Krasowsky, T. S., McMeeking, G. R., Wang, D., Sioutas, C., and Ban-Weiss, G. A.: Measurements of the impact of atmospheric aging on physical and optical properties of ambient black carbon particles in Los Angeles, Atmos. Environ., 142, 496-504, doi: 10.1016/j.atmosenv.2016.08.010, 2016.

Kumar, N. K., Corbin, J. C., Bruns, E. A., Massabó, D., Slowik, J. G., Drinovec, L., Močnik, G., Prati, P., Vlachou, A., Baltensperger, U., Gysel, M., El-Haddad, I., and Prévôt, A. S. H.: Production of particulate brown carbon during atmospheric aging of residential wood-burning emissions, Atmos. Chem. Phys., 18, 17843-17861, doi: 10.5194/acp-18-17843-2018, 2018.

Lack, D. A. and Cappa, C. D.: Impact of brown and clear carbon on light absorption enhancement, single scatter albedo and absorption wavelength dependence of black carbon, Atmos. Chem. Phys., 10, 4207-4220, doi: 10.5194/acp-10-4207-2010, 2010.

Lack, D. A., Langridge, J. M., Bahreini, R., Cappa, C. D., Middlebrook, A. M., and Schwarz, J. P.: Brown carbon and internal mixing in biomass burning particles, P Natl Acad Sci USA, 109, 14802-14807, doi: 10.1073/pnas.1206575109, 2012a.

Lack, D. A., Richardson, M. S., Law, D., Langridge, J. M., Cappa, C. D., McLaughlin, R. J., and Murphy, D. M.: Aircraft instrument for comprehensive characterization of aerosol optical properties, Part 2: black and brown carbon absorption and absorption enhancement measured with photo acoustic spectroscopy, Aerosol. Sci. Technol., 46, 555-568, doi: 10.1080/02786826.2011.645955, 2012b.

Lack, D. A. and Langridge, J. M.: On the attribution of black and brown carbon light absorption using the Ångström exponent, Atmos. Chem. Phys., 13, 10535-10543, doi: 10.5194/acp-13-10535-2013, 2013.

Lambe, A. T., Cappa, C. D., Massoli, P., Onasch, T. B., Forestieri, S. D., Martin, A. T., Cummings, M. J., Croasdale, D. R., Brune, W. H., Worsnop, D. R., and Davidovits, P.: Relationship between Oxidation Level and Optical Properties of Secondary Organic Aerosol, Environ. Sci. Technol., 47, 6349-6357, doi: 10.1021/es401043j, 2013.

Lan, Z.-J., Huang, X.-F., Yu, K.-Y., Sun, T.-L., Zeng, L.-W., and Hu, M.: Light absorption of black carbon aerosol and its enhancement by mixing state in an urban atmosphere in South China, Atmos. Environ., 69, 118-123, doi: 10.1016/j.atmosenv.2012.12.009, 2013.

Laskin, A., Laskin, J., and Nizkorodov, S. A.: Chemistry of Atmospheric Brown Carbon, Chemical Reviews, 115, 4335-4382, doi: 10.1021/cr5006167, 2015.

Lau, K. M., Kim, M. K., and Kim, K. M.: Asian summer monsoon anomalies induced by aerosol direct forcing: the role of the Tibetan Plateau, Climate Dynamics, 26, 855-864, doi: 10.1007/s00382-006-0114-z, 2006.

Lee, A. K. Y., Rivellini, L.-H., Chen, C.-L., Liu, J., Price, D., Betha, R., Russell, L. M., Zhang, X., and Cappa, C. D.: Influences of primary emission and secondary coating formation on the particle diversity and mixing state of black carbon particles, Environ. Sci. Technol., 53, 9429-9438, doi: 10.1021/acs.est.9b03064, 2019.

Lee, B. P., Li, Y. J., Yu, J. Z., Louie, P. K. K., and Chan, C. K.: Characteristics of submicron particulate matter at the urban roadside in downtown Hong Kong—Overview of 4 months of continuous high-resolution aerosol mass spectrometer measurements, J. Geophys. Res., 120, 7040-7058, doi: 10.1002/2015jd023311, 2015.

Lee, H. J., Aiona, P. K., Laskin, A., Laskin, J., and Nizkorodov, S. A.: Effect of Solar Radiation on the Optical Properties and Molecular Composition of Laboratory Proxies of Atmospheric Brown Carbon, Environ. Sci. Technol., 48, 10217-10226, doi: 10.1021/es502515r, 2014.

Lefevre, G., Yon, J., Bouvier, M., Liu, F., and Coppalle, A.: Impact of Organic Coating on Soot Angular and Spectral Scattering Properties, Environ. Sci. Technol., 53, 6383-6391, doi: 10.1021/acs.est.8b05482, 2019.

Levin, E. J. T., McMeeking, G. R., Carrico, C. M., Mack, L. E., Kreidenweis, S. M., Wold, C. E., Moosmüller, H., Arnott, W. P., Hao, W. M., Collett Jr., J. L., and Malm, W. C.: Biomass burning smoke aerosol properties measured during Fire Laboratory at

https://doi.org/10.5194/acp-2019-654
Preprint. Discussion started: 4 November 2019

Missoula Experiments (FLAME), J. Geophys. Res., 115, doi: 10.1029/2009jd013601, 2010.

Levy II, H., Mahlman, J. D., Moxim, W. J., and Liu, S. C.: Tropospheric ozone: The role of transport, J. Geophys. Res., 90, 3753-3772, doi: 10.1029/JD090iD02p03753, 1985.

Lewis, K., Arnott, W. P., Moosmüller, H., and Wold, C. E.: Strong spectral variation of biomass smoke light absorption and single scattering albedo observed with a novel dual-wavelength photoacoustic instrument, J. Geophys. Res., 113, D16203, doi: 10.1029/2007jd009699, 2008.

Li, C., He, Q., Schade, J., Passig, J., Zimmermann, R., Meidan, D., Laskin, A., and Rudich, Y.: Dynamic changes in optical and chemical properties of tar ball aerosols by atmospheric photochemical aging, Atmos. Chem. Phys., 19, 139-163, doi: 10.5194/acp-19-139-2019, 2019a.

Li, G.-L., Sun, L., Ho, K.-F., Wong, K.-C., and Ning, Z.: Implication of Light Absorption Enhancement and Mixing State of Black Carbon (BC) by Coatings in Hong Kong, Aerosol. Air. Qual. Res., 18, 2753-2763, doi: 10.4209/aaqr.2017.11.0473, 2018a.

Li, K., Ye, X., Pang, H., Lu, X., Chen, H., Wang, X., Yang, X., Chen, J., and Chen, Y.: Temporal variations in the hygroscopicity and mixing state of black carbon aerosols in a polluted megacity area, Atmos. Chem. Phys., 18, 15201-15218, doi: 10.5194/acp-18-15201-2018, 2018b.

Li, L., Huang, Z., Dong, J., Li, M., Gao, W., Nian, H., Fu, Z., Zhang, G., Bi, X., Cheng, P., and Zhou, Z.: Real time bipolar time-of-flight mass spectrometer for analyzing single aerosol particles, International Journal of Mass Spectrometry, 303, 118-124, doi: 10.1016/j.ijms.2011.01.017, 2011.

Li, M., Bao, F., Zhang, Y., Song, W., Chen, C., and Zhao, J.: Role of elemental carbon in the photochemical aging of soot, Proceedings of the National Academy of Sciences, 115, 7717-7722, doi: 10.1073/pnas.1804481115, 2018c.

Li, S., Zhu, M., Yang, W., Tang, M., Huang, X., Yu, Y., Fang, H., Yu, X., Yu, Q., Fu, X., Song, W., Zhang, Y., Bi, X., and Wang, X.: Filter-based measurement of light absorption by brown carbon in PM2.5 in a megacity in South China, Sci.Total.Environ., 633, 1360-1369, doi: 10.1016/j.scitotenv.2018.03.235, 2018d.

Li, Y. J., Sun, Y., Zhang, Q., Li, X., Li, M., Zhou, Z., and Chan, C. K.: Real-time chemical characterization of atmospheric particulate matter in China: A review, Atmos. Environ., 158, 270-304, doi: 10.1016/j.atmosenv.2017.02.027, 2017.

Li, Z., Tan, H., Zheng, J., Liu, L., Qin, Y., Wang, N., Li, F., Li, Y., Cai, M., Ma, Y., and Chan, C. K.: Light absorption property and potential source of particulate brown carbon in the Pearl River Delta region of China, Atmos. Chem. Phys. Discuss., 2019, 1-37, doi: 10.5194/acp-2018-1331, 2019b.

Liang, C., Pankow, J. F., Odum, J. R., and Seinfeld, J. H.: Gas/Particle Partitioning of Semivolatile Organic Compounds To Model Inorganic, Organic, and Ambient Smog Aerosols, Environ. Sci. Technol., 31, 3086-3092, doi: 10.1021/es9702529, 1997.

Lin, P., Laskin, J., Nizkorodov, S. A., and Laskin, A.: Revealing Brown Carbon Chromophores Produced in Reactions of Methylglyoxal with Ammonium Sulfate, Environ. Sci. Technol., 49, 14257-14266, doi: 10.1021/acs.est.5b03608, 2015.

Lin, P., Aiona, P. K., Li, Y., Shiraiwa, M., Laskin, J., Nizkorodov, S. A., and Laskin, A.: Molecular Characterization of Brown Carbon in Biomass Burning Aerosol Particles, Environ. Sci. Technol., 50, 11815-11824, doi: 10.1021/acs.est.6b03024, 2016.

Liu, B., Ma, Y., Gong, W., Zhang, M., and Shi, Y.: The relationship between black carbon and atmospheric boundary layer height, Atmospheric Pollution Research, 10, 65-72, doi: 10.1016/j.apr.2018.06.007, 2019a.

Liu, D., Allan, J. D., Young, D. E., Coe, H., Beddows, D., Fleming, Z. L., Flynn, M. J., Gallagher, M. W., Harrison, R. M., Lee, J., Prevot, A. S. H., Taylor, J. W., Yin, J., Williams, P. I., and Zotter, P.: Size distribution, mixing state and source apportionment of black carbon aerosol in London during wintertime, Atmos. Chem. Phys., 14, 10061-10084, doi: 10.5194/acp-14-10061-2014, 2014.

Liu, D., Whitehead, J., Alfarra, M. R., Reyes-Villegas, E., Spracklen, D. V., Reddington, C. L., Kong, S., Williams, P. I., Ting, Y.-C., Haslett, S., Taylor, J. W., Flynn, M. J., Morgan, W. T., McFiggans, G., Coe, H., and Allan, J. D.: Black-carbon absorption enhancement in the atmosphere determined by particle mixing state, Nature Geosci, 10, 184-188, doi: 10.1038/ngeo2901, 2017a.

Liu, F., Yon, J., and Bescond, A.: On the radiative properties of soot aggregates – Part 2: Effects of coating, Journal of Quantitative Spectroscopy and Radiative Transfer, 172, 134-145, doi: 10.1016/j.jqsrt.2015.08.005, 2016a.

Liu, H., Pan, X., Liu, D., Liu, X., Chen, X., Tian, Y., Sun, Y., Fu, P., and Wang, Z.: Mixing characteristics of refractory black carbon aerosols determined by a tandem CPMA-SP2 system at an urban site in Beijing, Atmos. Chem. Phys. Discuss., 2019, 1-25, doi: 10.5194/acp-2019-244, 2019b.

https://doi.org/10.5194/acp-2019-654
Preprint. Discussion started: 4 November 2019

Liu, J., Lin, P., Laskin, A., Laskin, J., Kathmann, S. M., Wise, M., Caylor, R., Imholt, F., Selimovic, V., and Shilling, J. E.: Optical properties and aging of light-absorbing secondary organic aerosol, Atmos. Chem. Phys., 16, 12815-12827, doi: 10.5194/acp-16-12815-2016, 2016b.

Liu, J., Wu, D., Fan, S., Mao, X., and Chen, H.: A one-year, on-line, multi-site observational study on water-soluble inorganic ions in PM2.5 over the Pearl River Delta region, China, Sci.Total.Environ., 601-602, 1720-1732, doi: 10.1016/j.scitotenv.2017.06.039, 2017b.

Liu, S., Aiken, A. C., Gorkowski, K., Dubey, M. K., Cappa, C. D., Williams, L. R., Herndon, S. C., Massoli, P., Fortner, E. C., Chhabra, P. S., Brooks, W. A., Onasch, T. B., Jayne, J. T., Worsnop, D. R., China, S., Sharma, N., Mazzoleni, C., Xu, L., Ng, N. L., Liu, D., Allan, J. D., Lee, J. D., Fleming, Z. L., Mohr, C., Zotter, P., Szidat, S., and Prevot, A. S. H.: Enhanced light absorption by mixed source black and brown carbon particles in UK winter, Nature Communications, 6, doi: 10.1038/ncomms9435, 2015.

Liu, S. C.: Possible effects on fropospheric O 3 and OH due to No emissions, Geophys. Res. Lett., 4, 325-328, doi: 10.1029/GL004i008p00325, 1977.

Lund, M. T., Samset, B. H., Skeie, R. B., Watson-Parris, D., Katich, J. M., Schwarz, J. P., and Weinzierl, B.: Short Black Carbon lifetime inferred from a global set of aircraft observations, npj Climate and Atmospheric Science, 1, 31, doi: 10.1038/s41612-018-0040-x, 2018.

Ma, X., Zangmeister, C. D., Gigault, J., Mulholland, G. W., and Zachariah, M. R.: Soot aggregate restructuring during water processing, J. Aerosol. Sci., 66, 209-219, doi: 10.1016/j.jaerosci.2013.08.001, 2013.

Martinsson, J., Eriksson, A. C., Nielsen, I. E., Malmborg, V. B., Ahlberg, E., Andersen, C., Lindgren, R., Nyström, R., Nordin, E. Z., Brune, W. H., Svenningsson, B., Swietlicki, E., Boman, C., and Pagels, J. H.: Impacts of Combustion Conditions and Photochemical Processing on the Light Absorption of Biomass Combustion Aerosol, Environ. Sci. Technol., 49, 14663-14671, doi: 10.1021/acs.est.5b03205, 2015.

Matsui, H., Hamilton, D. S., and Mahowald, N. M.: Black carbon radiative effects highly sensitive to emitted particle size when resolving mixing-state diversity, Nature Communications, 9, 3446, doi: 10.1038/s41467-018-05635-1, 2018.

McMeeking, G. R., Kreidenweis, S. M., Baker, S., Carrico, C. M., Chow, J. C., Collett, J. L., Hao, W. M., Holden, A. S., Kirchstetter, T. W., Malm, W. C., Moosmüller, H., Sullivan, A. P., and Wold, C. E.: Emissions of trace gases and aerosols during the open combustion of biomass in the laboratory, J. Geophys. Res., 114, doi: 10.1029/2009JD011836, 2009.

McMeeking, G. R., Fortner, E., Onasch, T. B., Taylor, J. W., Flynn, M., Coe, H., and Kreidenweis, S. M.: Impacts of nonrefractory material on light absorption by aerosols emitted from biomass burning, J. Geophys. Res., 119, 12,272-212,286, doi: 10.1002/2014JD021750, 2014.

Menon, S., Hansen, J., Nazarenko, L., and Luo, Y.: Climate Effects of Black Carbon Aerosols in China and India, Science, 297, 2250-2253, doi: 10.1126/science.1075159, 2002.

Metcalf, A. R., Loza, C. L., Coggon, M. M., Craven, J. S., Jonsson, H. H., Flagan, R. C., and Seinfeld, J. H.: Secondary Organic Aerosol Coating Formation and Evaporation: Chamber Studies Using Black Carbon Seed Aerosol and the Single-Particle Soot Photometer, Aerosol. Sci. Technol., 47, 326-347, doi: 10.1080/02786826.2012.750712, 2013.

Millet, D. B., Donahue, N. M., Pandis, S. N., Polidori, A., Stanier, C. O., Turpin, B. J., and Goldstein, A. H.: Atmospheric volatile organic compound measurements during the Pittsburgh Air Quality Study: Results, interpretation, and quantification of primary and secondary contributions, J. Geophys. Res., 110, D07S07, doi: 10.1029/2004jd004601, 2005.

Ming, J., Cachier, H., Xiao, C., Qin, D., Kang, S., Hou, S., and Xu, J.: Black carbon record based on a shallow Himalayan ice core and its climatic implications, Atmos. Chem. Phys., 8, 1343-1352, doi: 10.5194/acp-8-1343-2008, 2008.

Moffet, R. C. and Prather, K. A.: In-situ measurements of the mixing state and optical properties of soot with implications for radiative forcing estimates, P Natl Acad Sci USA, 106, 11872-11877, doi: 10.1073/pnas.0900040106, 2009.

Mohr, C., Huffman, J. A., Cubison, M. J., Aiken, A. C., Docherty, K. S., Kimmel, J. R., Ulbrich, I. M., Hannigan, M., and Jimenez, J. L.: Characterization of Primary Organic Aerosol Emissions from Meat Cooking, Trash Burning, and Motor Vehicles with High-Resolution Aerosol Mass Spectrometry and Comparison with Ambient and Chamber Observations, Environ. Sci. Technol., 43, 2443-2449, doi: 10.1021/es8011518, 2009.

Moise, T., Flores, J. M., and Rudich, Y.: Optical Properties of Secondary Organic Aerosols and Their Changes by Chemical

https://doi.org/10.5194/acp-2019-654
Preprint. Discussion started: 4 November 2019

Processes, Chemical Reviews, 115, 4400-4439, doi: 10.1021/cr5005259, 2015.

Moosmüller, H., Chakrabarty, R. K., Ehlers, K. M., and Arnott, W. P.: Absorption Angstrom coefficient, brown carbon, and aerosols: basic concepts, bulk matter, and spherical particles, Atmos. Chem. Phys., 11, 1217-1225, doi: 10.5194/acp-11-1217-2011, 2011.

Nenes, A., Conant, W. C., and Seinfeld, J. H.: Black carbon radiative heating effects on cloud microphysics and implications for the aerosol indirect effect 2. Cloud microphysics, J. Geophys. Res., 107, AAC 24-21-AAC 24-11, doi: 10.1029/2002jd002101, 2002.

Nordmann, S., Cheng, Y. F., Carmichael, G. R., Yu, M., Denier van der Gon, H. A. C., Zhang, Q., Saide, P. E., Pöschl, U., Su, H., Birmili, W., and Wiedensohler, A.: Atmospheric black carbon and warming effects influenced by the source and absorption enhancement in central Europe, Atmos. Chem. Phys., 14, 12683-12699, doi: 10.5194/acp-14-12683-2014, 2014.

Pathak, R., Donahue, N. M., and Pandis, S. N.: Ozonolysis of β-Pinene: Temperature Dependence of Secondary Organic Aerosol Mass Fraction, Environ. Sci. Technol., 42, 5081-5086, doi: 10.1021/es070721z, 2008.

Pei, X., Hallquist, M., Eriksson, A. C., Pagels, J., Donahue, N. M., Mentel, T., Svenningsson, B., Brune, W., and Pathak, R. K.: Morphological transformation of soot: investigation of microphysical processes during the condensation of sulfuric acid and limonene ozonolysis product vapors, Atmos. Chem. Phys., 18, 9845-9860, doi: 10.5194/acp-18-9845-2018, 2018.

Peng, J., Hu, M., Guo, S., Du, Z., Zheng, J., Shang, D., Levy Zamora, M., Zeng, L., Shao, M., Wu, Y.-S., Zheng, J., Wang, Y., Glen, C. R., Collins, D. R., Molina, M. J., and Zhang, R.: Markedly enhanced absorption and direct radiative forcing of black carbon under polluted urban environments, Proceedings of the National Academy of Sciences, 113, 4266-4271, doi: 10.1073/pnas.1602310113, 2016.

Peng, J., Hu, M., Guo, S., Du, Z., Shang, D., Zheng, J., Zheng, J., Zeng, L., Shao, M., Wu, Y., Collins, D., and Zhang, R.: Ageing and hygroscopicity variation of black carbon particles in Beijing measured by a quasi-atmospheric aerosol evolution study (QUALITY) chamber, Atmos. Chem. Phys., 17, 10333-10348, doi: 10.5194/acp-17-10333-2017, 2017.

Petit, J. E., Favez, O., Albinet, A., and Canonaco, F.: A user-friendly tool for comprehensive evaluation of the geographical origins of atmospheric pollution: Wind and trajectory analyses, Environ Modell Softw, 88, 183-187, doi: 10.1016/j.envsoft.2016.11.022, 2017.

Pokhrel, R. P., Wagner, N. L., Langridge, J. M., Lack, D. A., Jayarathne, T., Stone, E. A., Stockwell, C. E., Yokelson, R. J., and Murphy, S. M.: Parameterization of single-scattering albedo (SSA) and absorption Ångström exponent (AAE) with EC / OC for aerosol emissions from biomass burning, Atmos. Chem. Phys., 16, 9549-9561, doi: 10.5194/acp-16-9549-2016, 2016.

Qin, Y. M., Tan, H. B., Li, Y. J., Li, Z. J., Schurman, M. I., Liu, L., Wu, C., and Chan, C. K.: Chemical characteristics of brown carbon in atmospheric particles at a suburban site near Guangzhou, China, Atmos. Chem. Phys., 18, 16409-16418, doi: 10.5194/acp-18-16409-2018, 2018.

Radney, J. G., You, R., Zachariah, M. R., and Zangmeister, C. D.: Direct In Situ Mass Specific Absorption Spectra of Biomass Burning Particles Generated from Smoldering Hard and Softwoods, Environ. Sci. Technol., 51, 5622-5629, doi: 10.1021/acs.est.7b00810, 2017.

Ramanathan, V., Li, F., Ramana, M. V., Praveen, P. S., Kim, D., Corrigan, C. E., Nguyen, H., Stone, E. A., Schauer, J. J., Carmichael, G. R., Adhikary, B., and Yoon, S. C.: Atmospheric brown clouds: Hemispherical and regional variations in long-range transport, absorption, and radiative forcing, J. Geophys. Res., 112, doi: 10.1029/2006jd008124, 2007.

Reid, J. S., Eck, T. F., Christopher, S. A., Koppmann, R., Dubovik, O., Eleuterio, D. P., Holben, B. N., Reid, E. A., and Zhang, J.: A review of biomass burning emissions part III: intensive optical properties of biomass burning particles, Atmos. Chem. Phys., 5, 827-849, doi: 10.5194/acp-5-827-2005, 2005.

Roden, C. A., Bond, T. C., Conway, S., and Pinel, A. B. O.: Emission factors and real-time optical properties of particles emitted from traditional wood burning cookstoves, Environ. Sci. Technol., 40, 6750-6757, doi: 10.1021/es052080i, 2006.

Romonosky, D. E., Gomez, S. L., Lam, J., Carrico, C. M., Aiken, A. C., Chylek, P., and Dubey, M. K.: Optical Properties of Laboratory and Ambient Biomass Burning Aerosols: Elucidating Black, Brown, and Organic Carbon Components and Mixing Regimes, J. Geophys. Res., 124, 5088-5105, doi: 10.1029/2018jd029892, 2019.

Ruppel, M. M., Isaksson, I., Ström, J., Beaudon, E., Svensson, J., Pedersen, C. A., and Korhola, A.: Increase in elemental carbon values between 1970 and 2004 observed in a 300-year ice core from Holtedahlfonna (Svalbard), Atmos. Chem. Phys., 14, 11447-

11460, doi: 10.5194/acp-14-11447-2014, 2014.

Saathoff, H., Naumann, K. H., Schnaiter, M., Schöck, W., Möhler, O., Schurath, U., Weingartner, E., Gysel, M., and Baltensperger, U.: Coating of soot and (NH4)2SO4 particles by ozonolysis products of α-pinene, J. Aerosol. Sci., 34, 1297-1321, doi: 10.1016/S0021-8502(03)00364-1, 2003.

Saliba, G., Subramanian, R., Saleh, R., Ahern, A. T., Lipsky, E. M., Tasoglou, A., Sullivan, R. C., Bhandari, J., Mazzoleni, C., and Robinson, A. L.: Optical properties of black carbon in cookstove emissions coated with secondary organic aerosols: Measurements and modeling, Aerosol. Sci. Technol., 50, 1264-1276, doi: 10.1080/02786826.2016.1225947, 2016.

Santos, G. T. A. D., Santos, P. S. M., and Duarte, A. C.: Vanillic and syringic acids from biomass burning: Behaviour during Fenton-like oxidation in atmospheric aqueous phase and in the absence of light, J Hazard Mater, 313, 201-208, doi: 10.1016/j.jhazmat.2016.04.006, 2016a.

Santos, P. S. M. and Duarte, A. C.: Fenton-like oxidation of small aromatic acids from biomass burning in water and in the absence of light: Implications for atmospheric chemistry, Chemosphere, 119, 786-793, doi: 10.1016/j.chemosphere.2014.08.024, 2015.

Santos, P. S. M., Domingues, M. R. M., and Duarte, A. C.: Fenton-like oxidation of small aromatic acids from biomass burning in atmospheric water and in the absence of light: Identification of intermediates and reaction pathways, Chemosphere, 154, 599-603, doi: 10.1016/j.chemosphere.2016.04.015, 2016b.

Schmidl, C., Marr, I. L., Caseiro, A., Kotianová, P., Berner, A., Bauer, H., Kasper-Giebl, A., and Puxbaum, H.: Chemical characterisation of fine particle emissions from wood stove combustion of common woods growing in mid-European Alpine regions, Atmos. Environ., 42, 126-141, doi: 10.1016/j.atmosenv.2007.09.028, 2008.

Schnaiter, M., Linke, C., Mohler, O., Naumann, K. H., Saathoff, H., Wagner, R., Schurath, U., and Wehner, B.: Absorption amplification of black carbon internally mixed with secondary organic aerosol, J. Geophys. Res., 110, D19204, doi: 10.1029/2005JD006046, 2005.

Schwarz, J., Gao, R., Spackman, J., Watts, L., Thomson, D., Fahey, D., Ryerson, T., Peischl, J., Holloway, J., and Trainer, M.: Measurement of the mixing state, mass, and optical size of individual black carbon particles in urban and biomass burning emissions, Geophys. Res. Lett., 35, doi: 10.1029/2008GL033968, 2008a.

Schwarz, J. P., Spackman, J. R., Fahey, D. W., Gao, R. S., Lohmann, U., Stier, P., Watts, L. A., Thomson, D. S., Lack, D. A., Pfister, L., Mahoney, M. J., Baumgardner, D., Wilson, J. C., and Reeves, J. M.: Coatings and their enhancement of black carbon light absorption in the tropical atmosphere, J. Geophys. Res., 113, D03203, doi: 10.1029/2007JD009042, 2008b.

Shapiro, E. L., Szprengiel, J., Sareen, N., Jen, C. N., Giordano, M. R., and McNeill, V. F.: Light-absorbing secondary organic material formed by glyoxal in aqueous aerosol mimics, Atmos. Chem. Phys., 9, 2289-2300, doi: 10.5194/acp-9-2289-2009, 2009.

Shen, G., Chen, Y., Wei, S., Fu, X., Zhu, Y., and Tao, S.: Mass absorption efficiency of elemental carbon for source samples from residential biomass and coal combustions, Atmos. Environ., 79, 79-84, doi: 10.1016/j.atmosenv.2013.05.082, 2013.

Shiraiwa, M., Kondo, Y., Iwamoto, T., and Kita, K.: Amplification of Light Absorption of Black Carbon by Organic Coating, Aerosol. Sci. Technol., 44, 46-54, doi: 10.1080/02786820903357686, 2010.

Simoneit, B. R. T.: Biomass burning - A review of organic tracers for smoke from incomplete combustion, Appl Geochem, 17, 129-162, doi: 10.1016/S0883-2927(01)00061-0, 2002.

Sumlin, B. J., Pandey, A., Walker, M. J., Pattison, R. S., Williams, B. J., and Chakrabarty, R. K.: Atmospheric Photooxidation Diminishes Light Absorption by Primary Brown Carbon Aerosol from Biomass Burning, Environmental Science & Technology Letters, 4, 540-545, doi: 10.1021/acs.estlett.7b00393, 2017.

Tang, M., Alexander, J. M., Kwon, D., Estillore, A. D., Laskina, O., Young, M. A., Kleiber, P. D., and Grassian, V. H.: Optical and Physicochemical Properties of Brown Carbon Aerosol: Light Scattering, FTIR Extinction Spectroscopy, and Hygroscopic Growth, The Journal of Physical Chemistry A, 120, 4155-4166, doi: 10.1021/acs.jpca.6b03425, 2016.

Thamban, N. M., Tripathi, S. N., Moosakutty, S. P., Kuntamukkala, P., and Kanawade, V. P.: Internally mixed black carbon in the Indo-Gangetic Plain and its effect on absorption enhancement, Atmos Res, 197, 211-223, doi: 10.1016/j.atmosres.2017.07.007, 2017.

Tian, J., Wang, Q., Ni, H., Wang, M., Zhou, Y., Han, Y., Shen, Z., Pongpiachan, S., Zhang, N., Zhao, Z., Zhang, Q., Zhang, Y., Long, X., and Cao, J.: Emission Characteristics of Primary Brown Carbon Absorption From Biomass and Coal Burning:

https://doi.org/10.5194/acp-2019-654
Preprint. Discussion started: 4 November 2019

Development of an Optical Emission Inventory for China, J. Geophys. Res., 124, 1879-1893, doi: 10.1029/2018JD029352, 2019a.

Tian, M., Liu, Y., Yang, F., Zhang, L., Peng, C., Chen, Y., Shi, G., Wang, H., Luo, B., Jiang, C., Li, B., Takeda, N., and Koizumi, K.: Increasing importance of nitrate formation for heavy aerosol pollution in two megacities in Sichuan Basin, southwest China, Environ. Pollut., 250, 898-905, doi: 10.1016/j.envpol.2019.04.098, 2019b.

Turpin, B. J. and Huntzicker, J. J.: Identification of secondary organic aerosol episodes and quantitation of primary and secondary organic aerosol concentrations during SCAQS, Atmos. Environ., 29, 3527-3544, doi: 10.1016/1352-2310(94)00276-Q, 1995.

Ueda, S., Nakayama, T., Taketani, F., Adachi, K., Matsuki, A., Iwamoto, Y., Sadanaga, Y., and Matsumi, Y.: Light absorption and morphological properties of soot-containing aerosols observed at an East Asian outflow site, Noto Peninsula, Japan, Atmos. Chem. Phys., 16, 2525-2541, doi: 10.5194/acp-16-2525-2016, 2016.

Virkkula, A., Makela, T., Hillamo, R., Yli-Tuomi, T., Hirsikko, A., Hameri, K., and Koponen, I. K.: A simple procedure for correcting loading effects of aethalometer data, J. Air Waste Manage. Assoc., 57, 1214-1222, doi: 10.3155/1047-3289.57.10.1214, 2007.

Wang, J., Zhang, Q., Chen, M., Collier, S., Zhou, S., Ge, X., Xu, J., Shi, J., Xie, C., Hu, J., Ge, S., Sun, Y., and Coe, H.: First Chemical Characterization of Refractory Black Carbon Aerosols and Associated Coatings over the Tibetan Plateau (4730 m a.s.l), Environ. Sci. Technol., 51, 14072-14082, doi: 10.1021/acs.est.7b03973, 2017a.

Wang, J., Zhao, B., Wang, S., Yang, F., Xing, J., Morawska, L., Ding, A., Kulmala, M., Kerminen, V.-M., Kujansuu, J., Wang, Z., Ding, D., Zhang, X., Wang, H., Tian, M., Petäjä, T., Jiang, J., and Hao, J.: Particulate matter pollution over China and the effects of control policies, Sci.Total.Environ., 584-585, 426-447, doi: 10.1016/j.scitotenv.2017.01.027, 2017b.

Wang, Q., Huang, R., Zhao, Z., Cao, J., Ni, H., Tie, X., Zhu, C., Shen, Z., Wang, M., and Dai, W.: Effects of photochemical oxidation on the mixing state and light absorption of black carbon in the urban atmosphere of China, Environmental Research Letters, 12, 044012, doi: 10.1088/1748-9326/aa64ea, 2017c.

Wang, Q., Cao, J., Han, Y., Tian, J., Zhang, Y., Pongpiachan, S., Zhang, Y., Li, L., Niu, X., Shen, Z., Zhao, Z., Tipmanee, D., Bunsomboonsakul, S., Chen, Y., and Sun, J.: Enhanced light absorption due to the mixing state of black carbon in fresh biomass burning emissions, Atmos. Environ., 180, 184-191, doi: 10.1016/j.atmosenv.2018.02.049, 2018a.

Wang, Q., Cao, J., Han, Y., Tian, J., Zhu, C., Zhang, Y., Zhang, N., Shen, Z., Ni, H., Zhao, S., and Wu, J.: Sources and physicochemical characteristics of black carbon aerosol from the southeastern Tibetan Plateau: internal mixing enhances light absorption, Atmos. Chem. Phys., 18, 4639-4656, doi: 10.5194/acp-18-4639-2018, 2018b.

Wang, Q. Y., Huang, R. J., Cao, J. J., Han, Y. M., Wang, G. H., Li, G. H., Wang, Y. C., Dai, W. T., Zhang, R. J., and Zhou, Y. Q.: Mixing State of Black Carbon Aerosol in a Heavily Polluted Urban Area of China: Implications for Light Absorption Enhancement, Aerosol. Sci. Technol., 48, 689-697, doi: 10.1080/02786826.2014.917758, 2014.

Wang, Y. Q.: MeteoInfo: GIS software for meteorological data visualization and analysis, Meteorol. Appl., 21, 360-368, doi: 10.1002/met.1345, 2014.

Wang, Y. Q.: An Open Source Software Suite for Multi-Dimensional Meteorological Data Computation and Visualisation, Journal of Open Research Software, 7, 21, doi: 10.5334/jors.267, 2019.

Warren, B., Austin, R. L., and Cocker, D. R.: Temperature dependence of secondary organic aerosol, Atmos. Environ., 43, 3548-3555, doi: 10.1016/j.atmosenv.2009.04.011, 2009.

Wei, Y., Ma, L., Cao, T., Zhang, Q., Wu, J., Buseck, P. R., and Thompson, J. E.: Light Scattering and Extinction Measurements Combined with Laser-Induced Incandescence for the Real-Time Determination of Soot Mass Absorption Cross Section, Anal. Chem., 85, 9181-9188, doi: 10.1021/ac401901b, 2013.

Weyant, C. L., Shepson, P. B., Subramanian, R., Cambaliza, M. O. L., Heimburger, A., McCabe, D., Baum, E., Stirm, B. H., and Bond, T. C.: Black Carbon Emissions from Associated Natural Gas Flaring, Environ. Sci. Technol., 50, 2075-2081, doi: 10.1021/acs.est.5b04712, 2016.

Wilcox, E. M., Thomas, R. M., Praveen, P. S., Pistone, K., Bender, F. A.-M., and Ramanathan, V.: Black carbon solar absorption suppresses turbulence in the atmospheric boundary layer, Proceedings of the National Academy of Sciences, 113, 11794-11799, doi: 10.1073/pnas.1525746113, 2016.

Williams, M. A., Kumar, T. V. L., and Rao, D. N.: Characterizing black carbon aerosols in relation to atmospheric boundary layer

height during wet removal processes over a semi urban location, J. Atmos. Sol-terr. Phy., 182, 165-176, doi: 10.1016/j.jastp.2018.11.018, 2019.

Wong, J. P. S., Tsagkaraki, M., Tsiodra, I., Mihalopoulos, N., Violaki, K., Kanakidou, M., Sciare, J., Nenes, A., and Weber, R. J.: Atmospheric evolution of molecular-weight-separated brown carbon from biomass burning, Atmos. Chem. Phys., 19, 7319-7334, doi: 10.5194/acp-19-7319-2019, 2019.

Wu, C. and Yu, J. Z.: Determination of primary combustion source organic carbon-to-elemental carbon (OC/EC) ratio using ambient OC and EC measurements: secondary OC-EC correlation minimization method, Atmos. Chem. Phys., 16, 5453-5465, doi: 10.5194/acp-16-5453-2016, 2016.

Wu, C., Wu, D., and Yu, J. Z.: Quantifying black carbon light absorption enhancement with a novel statistical approach, Atmos. Chem. Phys., 18, 289-309, doi: 10.5194/acp-18-289-2018, 2018.

Wu, C. and Yu, J. Z.: Evaluation of linear regression techniques for atmospheric applications: the importance of appropriate weighting, Atmos. Meas. Tech., 11, 1233-1250, doi: 10.5194/amt-11-1233-2018, 2018.

Wu, C., Wu, D., and Yu, J. Z.: Estimation and Uncertainty Analysis of Secondary Organic Carbon Using One-Year of Hourly Organic and Elemental Carbon Data, J. Geophys. Res., 124, 2774-2795, doi: 10.1029/2018JD029290, 2019.

Xia, Y., Zhao, Y., and Nielsen, C. P.: Benefits of China's efforts in gaseous pollutant control indicated by the bottom-up emissions and satellite observations 2000–2014, Atmos. Environ., 136, 43-53, doi: 10.1016/j.atmosenv.2016.04.013, 2016.

Xie, C., Xu, W., Wang, J., Liu, D., Ge, X., Zhang, Q., Wang, Q., Du, W., Zhao, J., Zhou, W., Li, J., Fu, P., Wang, Z., Worsnop, D., and Sun, Y.: Light absorption enhancement of black carbon in urban Beijing in summer, Atmos. Environ., 213, 499-504, doi: 10.1016/j.atmosenv.2019.06.041, 2019.

Xie, S., Zhang, Y., Qi, L., and Tang, X.: Spatial distribution of traffic-related pollutant concentrations in street canyons, Atmos. Environ., 37, 3213-3224, doi: 10.1016/S1352-2310(03)00321-2, 2003.

Xu, J., Cui, T., Fowler, B., Fankhauser, A., Yang, K., Surratt, J. D., and McNeill, V. F.: Aerosol Brown Carbon from Dark Reactions of Syringol in Aqueous Aerosol Mimics, ACS Earth and Space Chemistry, 2, 608-617, doi: 10.1021/acsearthspacechem.8b00010, 2018a.

Xu, J., Wang, Q., Deng, C., McNeill, V. F., Fankhauser, A., Wang, F., Zheng, X., Shen, J., Huang, K., and Zhuang, G.: Insights into the characteristics and sources of primary and secondary organic carbon: High time resolution observation in urban Shanghai, Environ. Pollut., 233, 1177-1187, doi: 10.1016/j.envpol.2017.10.003, 2018b.

Xu, Q., Wang, S., Jiang, J., Bhattarai, N., Li, X., Chang, X., Qiu, X., Zheng, M., Hua, Y., and Hao, J.: Nitrate dominates the chemical composition of PM2.5 during haze event in Beijing, China, Sci.Total.Environ., doi: 10.1016/j.scitotenv.2019.06.294, 2019.

Xu, X., Zhao, W., Zhang, Q., Wang, S., Fang, B., Chen, W., Venables, D. S., Wang, X., Pu, W., Wang, X., Gao, X., and Zhang, W.: Optical properties of atmospheric fine particles near Beijing during the HOPE-J3A campaign, Atmos. Chem. Phys., 16, 6421-6439, doi: 10.5194/acp-16-6421-2016, 2016.

Xu, X., Zhao, W., Qian, X., Wang, S., Fang, B., Zhang, Q., Zhang, W., Venables, D. S., Chen, W., Huang, Y., Deng, X., Wu, B., Lin, X., Zhao, S., and Tong, Y.: Influence of photochemical aging on light absorption of atmospheric black carbon and aerosol single scattering albedo, Atmos. Chem. Phys., 18, 16829-16844, doi: 10.5194/acp-2018-59, 2018c.

Xue, H. X., Khalizov, A. F., Wang, L., Zheng, J., and Zhang, R. Y.: Effects of dicarboxylic acid coating on the optical properties of soot, Physical Chemistry Chemical Physics, 11, 7869-7875, doi: 10.1039/b904129j, 2009.

Xue, J., Yuan, Z., Lau, A. K. H., and Yu, J. Z.: Insights into factors affecting nitrate in PM2.5 in a polluted high NOx environment through hourly observations and size distribution measurements, J. Geophys. Res., 119, 4888-4902, doi: 10.1002/2013JD021108, 2014.

Yao, Z., Zhang, Y., Shen, X., Wang, X., Wu, Y., and He, K.: Impacts of temporary traffic control measures on vehicular emissions during the Asian Games in Guangzhou, China, J. Air Waste Manage. Assoc., 63, 11-19, doi: 10.1080/10962247.2012.724041, 2013.

Ye, Z., Qu, Z., Ma, S., Luo, S., Chen, Y., Chen, H., Chen, Y., Zhao, Z., Chen, M., and Ge, X.: A comprehensive investigation of aqueous-phase photochemical oxidation of 4-ethylphenol, Sci.Total.Environ., 685, 976-985, doi: 10.1016/j.scitotenv.2019.06.276, 2019.

Ying, Q., Feng, M., Song, D., Wu, L., Hu, J., Zhang, H., Kleeman, M. J., and Li, X.: Improve regional distribution and source

apportionment of PM2.5 trace elements in China using inventory-observation constrained emission factors, Sci.Total.Environ., 624, 355-365, doi: 10.1016/j.scitotenv.2017.12.138, 2018.

You, R., Radney, J. G., Zachariah, M. R., and Zangmeister, C. D.: Measured Wavelength-Dependent Absorption Enhancement of Internally Mixed Black Carbon with Absorbing and Nonabsorbing Materials, Environ. Sci. Technol., 50, 7982-7990, doi: 10.1021/acs.est.6b01473, 2016.

Zhang, G., Bi, X., Li, L., Chan, L. Y., Li, M., Wang, X., Sheng, G., Fu, J., and Zhou, Z.: Mixing state of individual submicron carbon-containing particles during spring and fall seasons in urban Guangzhou, China: a case study, Atmos. Chem. Phys., 13, 4723-4735, doi: 10.5194/acp-13-4723-2013, 2013.

Zhang, G., Han, B., Bi, X., Dai, S., Huang, W., Chen, D., Wang, X., Sheng, G., Fu, J., and Zhou, Z.: Characteristics of individual particles in the atmosphere of Guangzhou by single particle mass spectrometry, Atmos Res, 153, 286-295, doi: 10.1016/j.atmosres.2014.08.016, 2015.

Zhang, G. H., Bi, X. H., He, J. J., Chen, D. H., Chan, L. Y., Xie, G. W., Wang, X. M., Sheng, G. Y., Fu, J. M., and Zhou, Z.: Variation of secondary coatings associated with elemental carbon by single particle analysis, Atmos. Environ., 92, 162-170, doi: 10.1016/j.atmosenv.2014.04.018, 2014.

Zhang, R. Y., Khalizov, A. F., Pagels, J., Zhang, D., Xue, H. X., and McMurry, P. H.: Variability in morphology, hygroscopicity, and optical properties of soot aerosols during atmospheric processing, P Natl Acad Sci USA, 105, 10291-10296, doi: 10.1073/pnas.0804860105, 2008.

Zhang, X., Mao, M., Yin, Y., and Wang, B.: Absorption enhancement of aged black carbon aerosols affected by their microphysics: A numerical investigation, Journal of Quantitative Spectroscopy and Radiative Transfer, 202, 90-97, doi: 10.1016/j.jqsrt.2017.07.025, 2017.

Zhang, Y., Favez, O., Canonaco, F., Liu, D., Močnik, G., Amodeo, T., Sciare, J., Prévôt, A. S. H., Gros, V., and Albinet, A.: Evidence of major secondary organic aerosol contribution to lensing effect black carbon absorption enhancement, npj Climate and Atmospheric Science, 1, 47, doi: 10.1038/s41612-018-0056-2, 2018a.

Zhang, Y., Zhang, Q., Cheng, Y., Su, H., Li, H., Li, M., Zhang, X., Ding, A., and He, K.: Amplification of light absorption of black carbon associated with air pollution, Atmos. Chem. Phys., 18, 9879-9896, doi: 10.5194/acp-18-9879-2018, 2018b.

Zhong, M. and Jang, M.: Light absorption coefficient measurement of SOA using a UV–Visible spectrometer connected with an integrating sphere, Atmos. Environ., 45, 4263-4271, doi: 10.1016/j.atmosenv.2011.04.082, 2011.

Zhong, M. and Jang, M.: Dynamic light absorption of biomass-burning organic carbon photochemically aged under natural sunlight, Atmos. Chem. Phys., 14, 1517-1525, doi: 10.5194/acp-14-1517-2014, 2014.

Zhou, Y., Huang, X. H. H., Griffith, S. M., Li, M., Li, L., Zhou, Z., Wu, C., Meng, J., Chan, C. K., Louie, P. K. K., and Yu, J. Z.: A field measurement based scaling approach for quantification of major ions, organic carbon, and elemental carbon using a single particle aerosol mass spectrometer, Atmos. Environ., 143, 300-312, doi: 10.1016/j.atmosenv.2016.08.054, 2016.

https://doi.org/10.5194/acp-2019-654
Preprint. Discussion started: 4 November 2019

Atmospheric Chemistry and Physics Discussions

Table 1. Comparisons of three E_{abs} determination approaches.

Approach	Time resolution	Temporal coverage	E_{abs} determination	Instrument	Limitations
TD	minutes	months	$\boldsymbol{E_{abs}} = \frac{\sigma_{abs\_total}}{\sigma_{abs\_pri}}$	TD+PAS	TD temperature selection; denuded particle morphology different from emission
AFD	daily	years	$\boldsymbol{E_{abs}} = \frac{\sigma_{abs\_total}}{\sigma_{abs\_pri}}$	Filter sampler + off-line OCEC	labor intensive; only remove soluble coating
MAE+MRS	hourly	years	$\boldsymbol{E_{abs}} = \frac{MAE_t}{MAE_p}$	Aethalometer + online OCEC	MRS has minimum data points requirement, not suitable for a small dataset

https://doi.org/10.5194/acp-2019-654
Preprint. Discussion started: 4 November 2019

Atmospheric Chemistry and Physics Discussions

Table 2. Comparisons E_{abs} in various field studies.

Method	Location	Sampling duration	λ nm	E_{abs}	Reference
MAE	Guangzhou,China (Urban)	Jul-Sept 2017 Nov2017-Jan2018	520	1.51±0.50 1.29±0.28	This study
	Guangzhou,China (Suburban)	Feb 2012-Jan 2013	550	1.50±0.48	(Wu et al., 2018)
	Beijing, China (Suburban)	Nov 2014–Jan 2015	470	2.6–4.0	(Xu et al., 2016)
	Beijing, China (Urban)	Nov 2014	/	1.66-1.91	(Zhang et al., 2018b)
	Manchester, UK (Urban)	Oct2-Nov 2014	532	1.0–1.3	(Liu et al., 2017a)
	Paris, France (Urban)	Mar 2014–Mar 2017	880	1.53±0.39	(Zhang et al., 2018a)
	Kanpur, India (Urban)	Jan-Feb 2015	781	1.8	(Thamban et al., 2017)
	Nanjing, China (Suburban)	Nov 2012	532	1.6	(Cui et al., 2016a)
	Xi'an, China (Urban)	Dec 2012-Jan 2013	870	1.8	(Wang et al., 2014)
TD	Shouxian, China (Rural)	Jun-Jul 2016	532	2.3 ± 0.9	(Xu et al., 2018c)
	Beijing, China (Urban)	Jun 2017	630	1.59±0.26	(Xie et al., 2019)
	Sacramento, USA (Urban)	Jun-Jul 2010	532	1.06± 0.01	(Cappa et al., 2012)
	Fresno, USA (Urban)	Dec 2014-Jan 2015	532	1.22± 0.15	(Cappa et al., 2019)
	Fontana, USA (Urban)	July 2015	532	1.07± 0.22	
	Suzu, Japan	April-May 2013	532	1.06	(Ueda et al., 2016)
AFD	Jinan, China (Urban)	February 2014	678	2.07± 0.72	(Chen et al., 2017)
	Yuncheng, China (Rural)	Jun-Jul 2014	678	2.25± 0.55	(Cui et al., 2016b)

https://doi.org/10.5194/acp-2019-654
Preprint. Discussion started: 4 November 2019

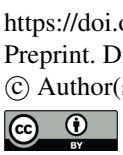

Atmospheric Chemistry and Physics Discussions

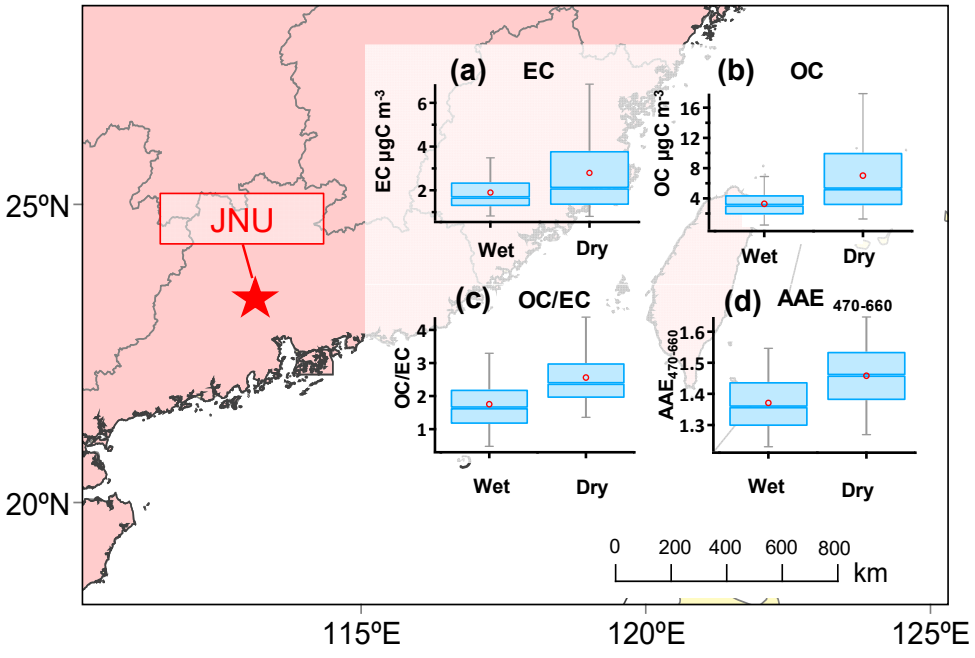

1185 **Figure 1.** The location of the observation site. (a), (b), (c) and (d) show the box plot of EC, OC, OC/EC and $AAE_{470\text{-}660}$, respectively. Red circles represent the seasonal average. The line inside the box indicates the median. Upper and lower boundaries of the box represent the 75th and the 25th percentiles; the whiskers above and below each box represent the 95th and 5th percentiles.

https://doi.org/10.5194/acp-2019-654
Preprint. Discussion started: 4 November 2019

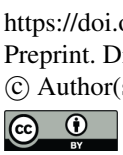

Atmospheric Chemistry and Physics Discussions

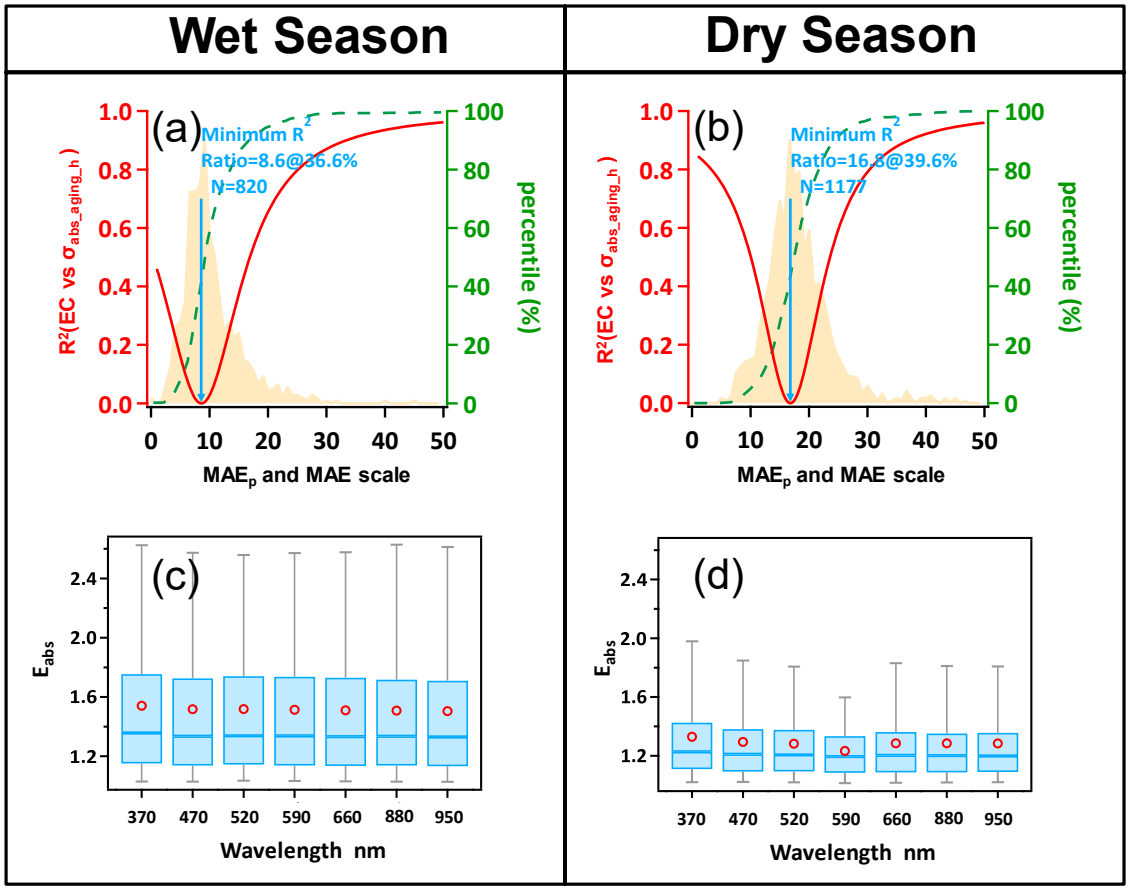

Figure 2. E_{abs} determination by MRS. (a) Wet season MAE_p determined by MRS at 520 nm. The red curve represents the correlation coefficient (R^2) between hypothetical σ_{abs_aging} (σ_{abs_total} – EC * MAE_p) and EC mass as a function of MAE_{p_h}. The shaded area in light tan represents the frequency distribution of observed MAE. The dashed green line is the cumulative distribution of observed MAE. (b) same as (a) but for dry season. (c) Spectral E_{abs} determined by MRS in wet season. Red circles represent the average values. The line inside the box indicates the median. Upper and lower boundaries of the box represent the 75th and the 25th percentiles; the whiskers above and below each box represent the 95th and 5th percentiles. (d) Spectral E_{abs} in dry season.

https://doi.org/10.5194/acp-2019-654
Preprint. Discussion started: 4 November 2019

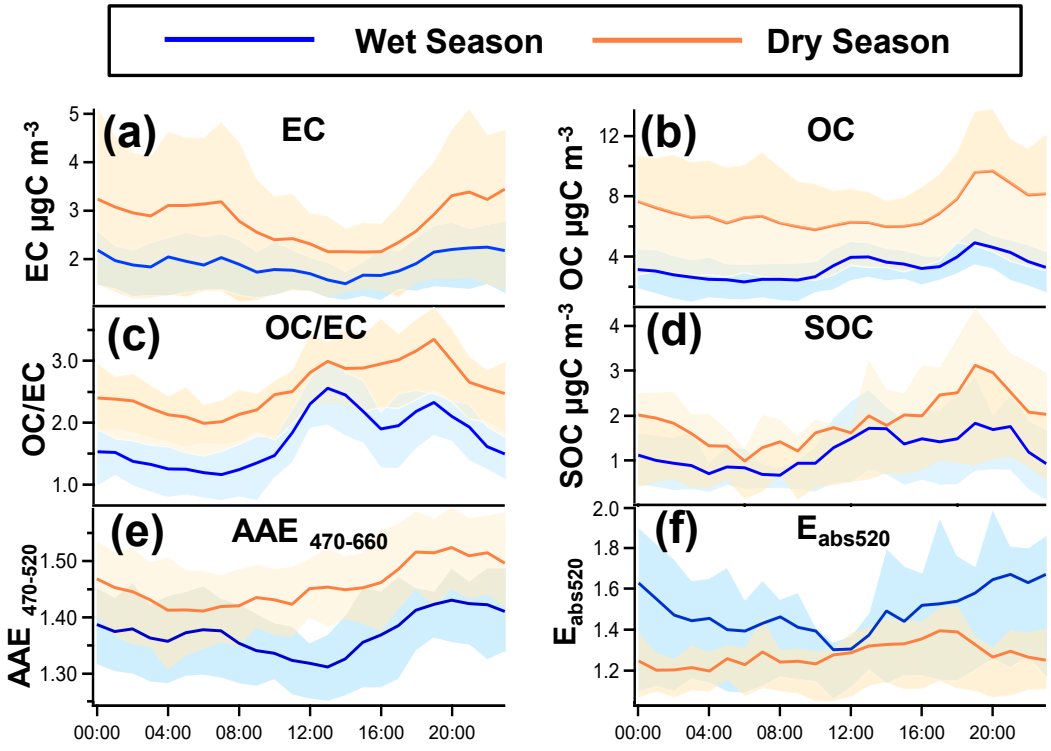

Figure 3. Diurnal pattern carbonaceous aerosols in wet and dry season. The solid lines represent hourly averages and the shaded areas represent 25th% and 75th% percentile. (a) EC. (b) OC. (c) OC/EC ratio. (d) SOC. (e) $AAE_{470\text{-}660}$. (f) E_{abs520}.

https://doi.org/10.5194/acp-2019-654
Preprint. Discussion started: 4 November 2019

Atmospheric Chemistry and Physics Discussions

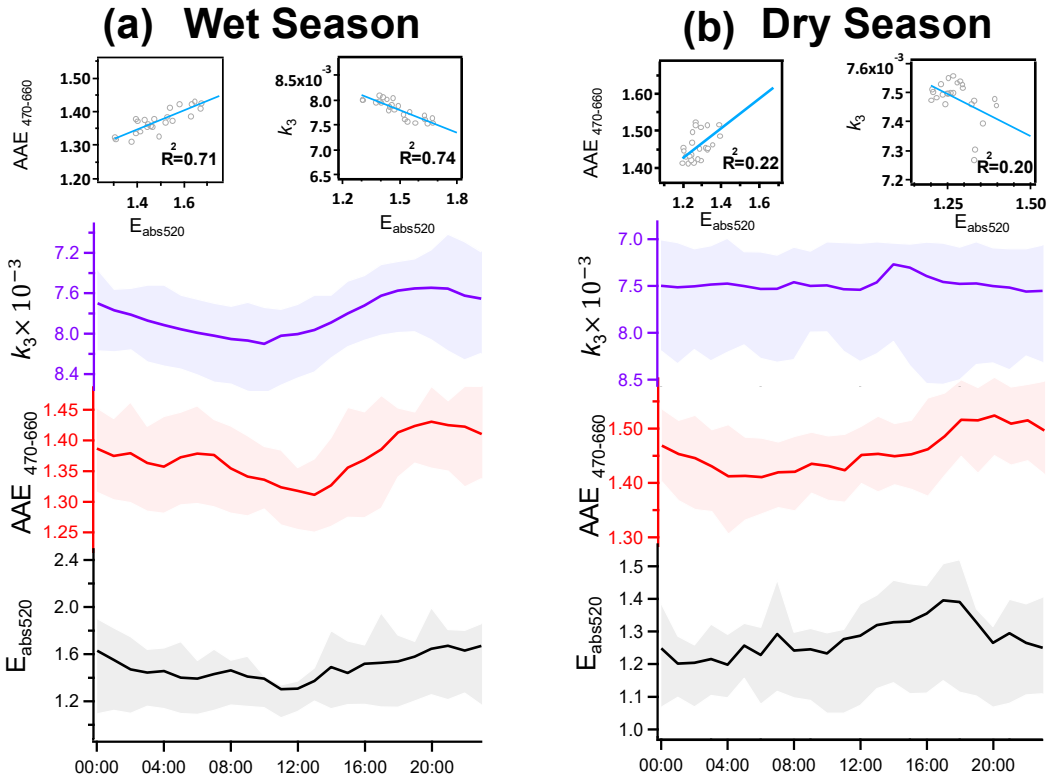

Figure 4. diurnal patterns of E_{abs520} $AAE_{470-660}$ and k_3. The solid lines represent hourly averages and the shaded areas represent 25th% and 75th% percentile. (a) Wet season. (b) Dry season. It should be noted that the k_3 was shown on an inverted scale.

https://doi.org/10.5194/acp-2019-654
Preprint. Discussion started: 4 November 2019

Atmospheric Chemistry and Physics Discussions

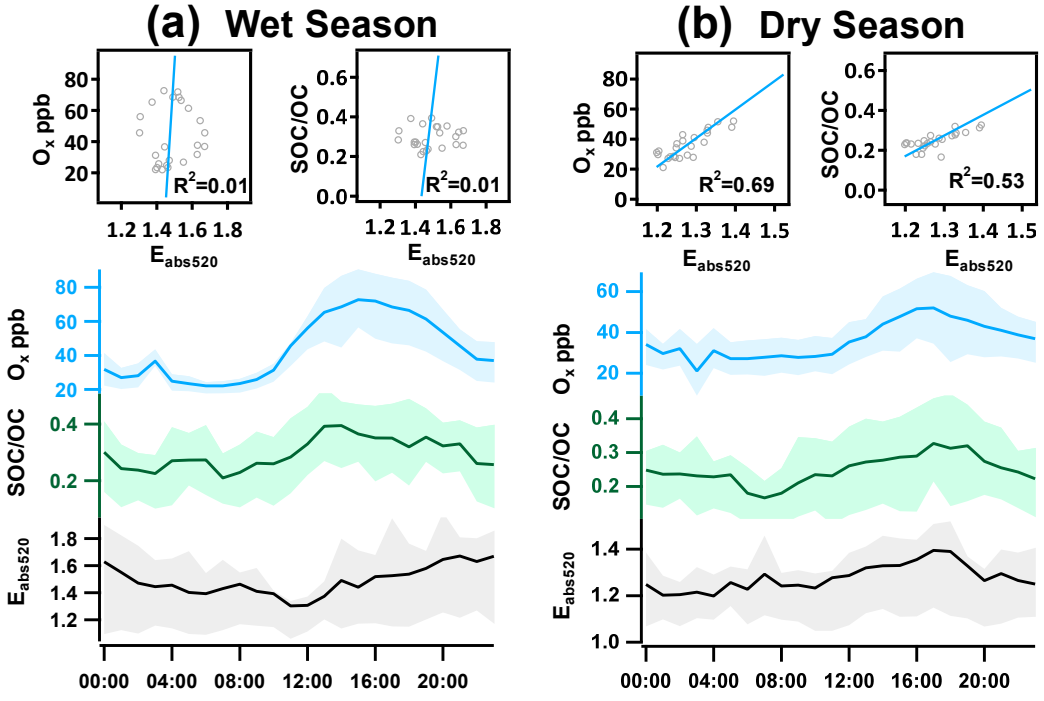

Figure 5. The effect of secondary process on E_{abs520}. (a) Diurnal pattern of E_{abs520} and O_x in wet season. The solid lines represent hourly averages and the shaded areas represent 25th% and 75th% percentile. (b) Same as (a) but in dry season.

https://doi.org/10.5194/acp-2019-654
Preprint. Discussion started: 4 November 2019

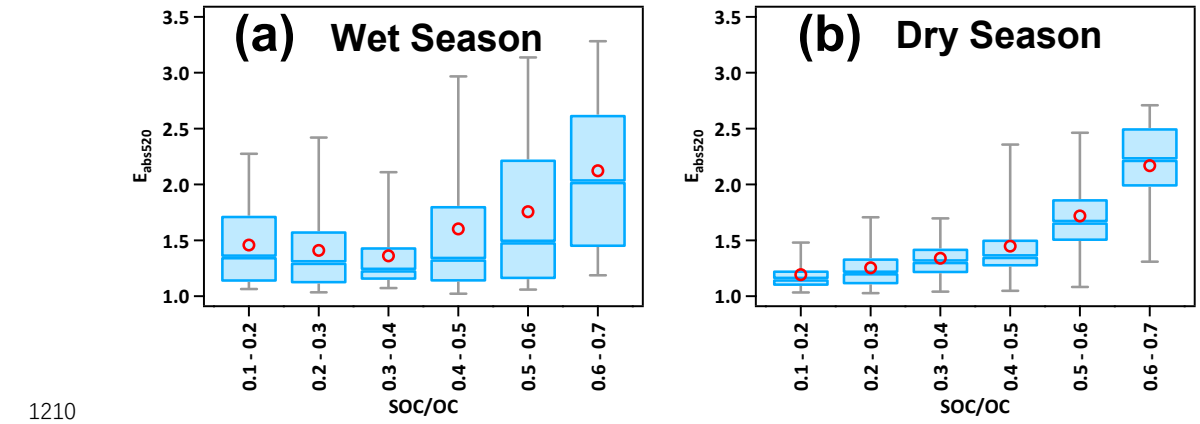

Figure 6. E_{abs520} dependency on SOC/OC ratio. (a) Wet season (b) Dry season. Red circles represent the average values. The line inside the box indicates the median. Upper and lower boundaries of the box represent the 75th and the 25th percentiles; the whiskers above and below each box represent the 95th and 5th percentiles.

https://doi.org/10.5194/acp-2019-654
Preprint. Discussion started: 4 November 2019

Atmospheric Chemistry and Physics Discussions

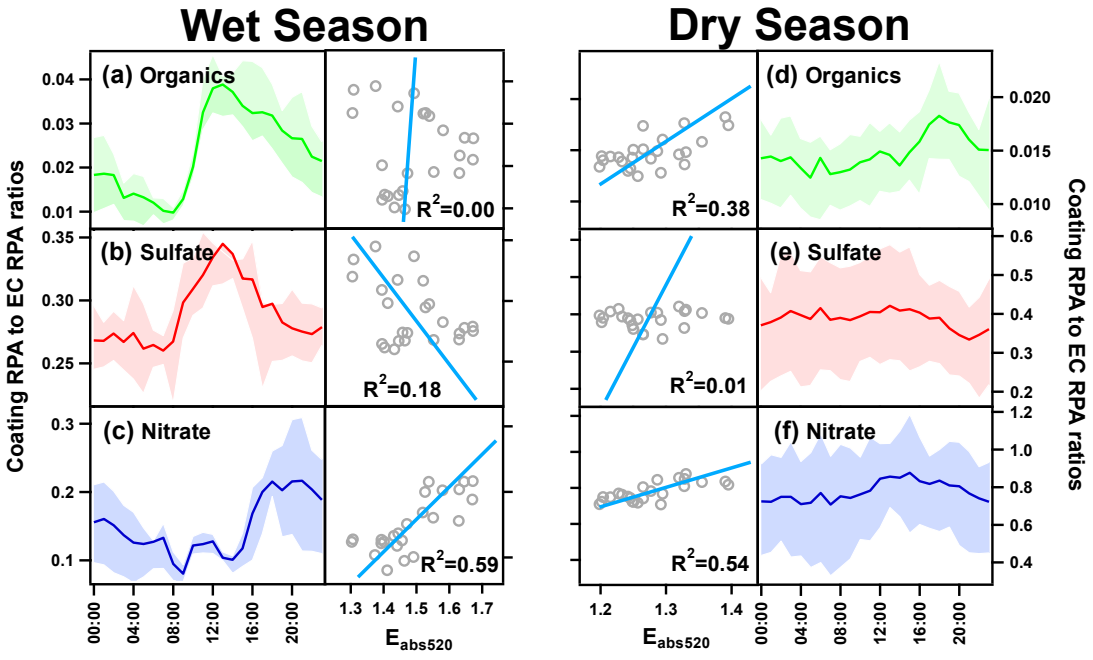

Figure 7. Diurnal variations of coating (including organics, sulfate and nitrate) RPA to EC RPA ratios of EC-aged particles measured by SPAMS in wet and dry seasons. The solid lines represent hourly averages and the shaded areas represent 25th% and 75th% percentile. (a) ~(c) In wet season, organics, nitrate and sulfate RPA to EC PRA ratios. The scatter plots show the corresponding correlations with E_{abs520}. The scatter plots share the same y axis scale with the diurnal plots. (d) ~(f) are the same as (a) ~(c) but for the dry season. Following ions are used: EC (m/z +12$[C]^+$, +24$[C_2]^+$, +36$[C_3]^+$, +48$[C_4]^+$), organics (m/z +43$[C_2H_3O]^+$), sulfate (m/z -97 $[HSO_4]^-$, -80$[SO_3]^-$) and nitrate m/z -62 $[HNO_3]^-$, -46$[NO_2]^-$).